united nations
educational, scientific
and cultural
organization

international atomic
energy agency

the
abdus salam
international centre for theoretical physics

SMR.1135 - 6

THIRD WORKSHOP ON
THIN FILMS PHYSICS AND TECHNOLOGY
(8 - 24 MARCH 1999)
including
TOPICAL CONFERENCE ON
MICROSTRUCTURE AND SURFACE MORPHOLOGY
EVOLUTION IN THIN FILMS
(24 - 26 MARCH 1999)

"Electron microscopy, high energy electron diffraction and electron energy loss spectroscopy of nanoparticles and thin films"

Miguel YACAMAN
Universidad Nacional Autonoma de Mexico
Instituto de Fisica
Apdo. Post. 20-364
Delegacion Alvaro Obregon
01000 Mexico City
MEXICO

Thin films

- Continuos single crystalline films.
- Polycrystalline films
- Discontinuous films discrete grains
- Multilayered films
- Substrate + Films


50nm

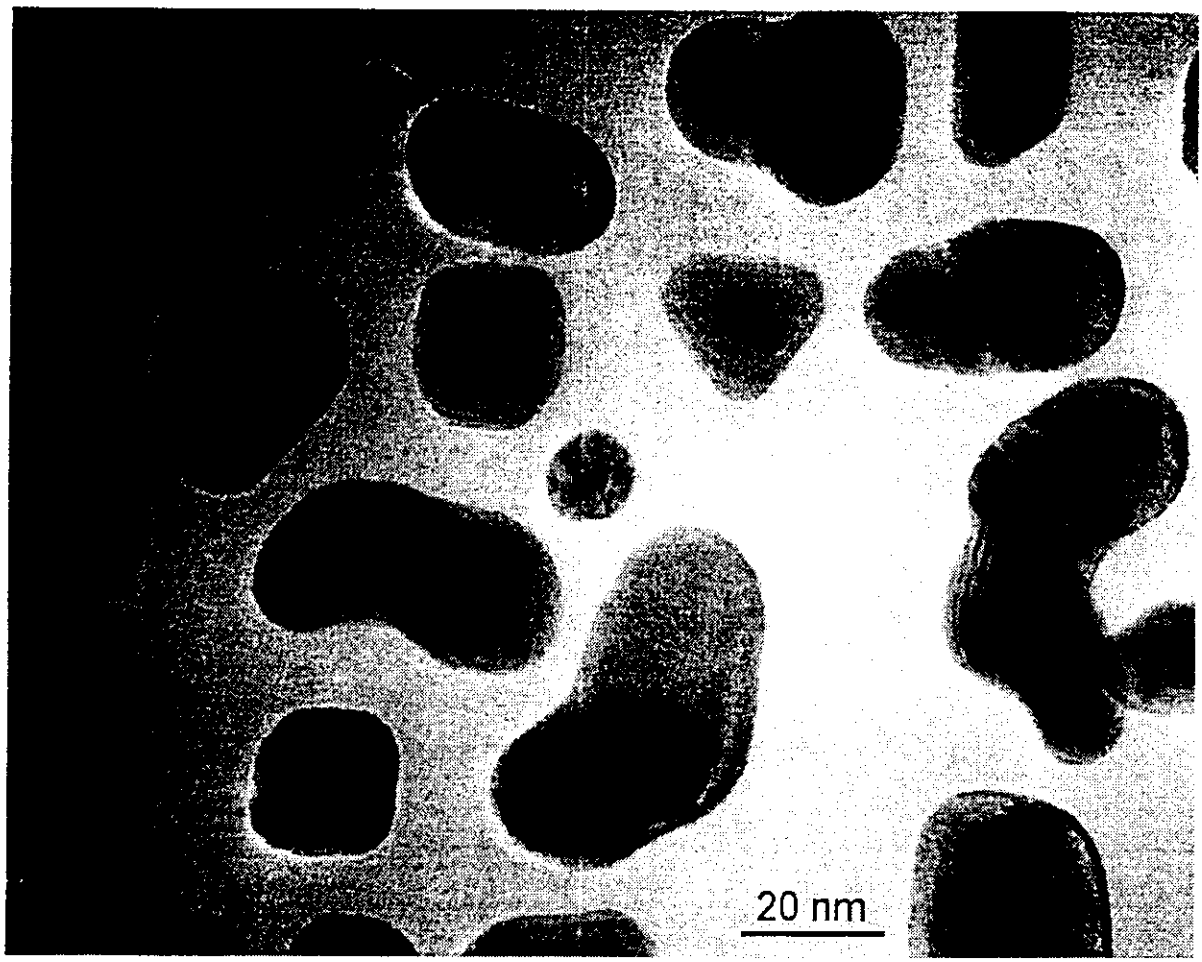
20 nm

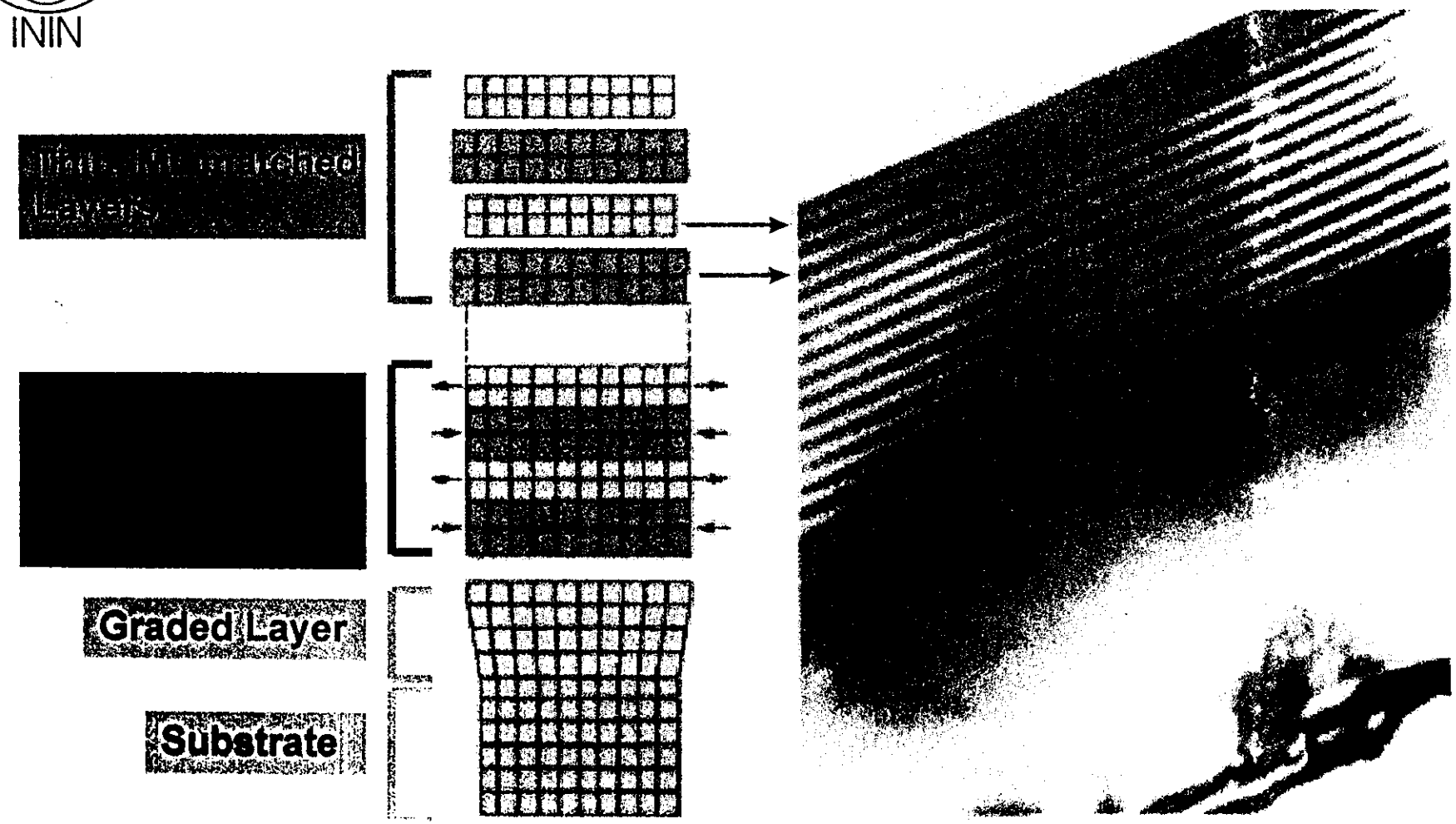

Strained-layer superlattices for band gap engineering

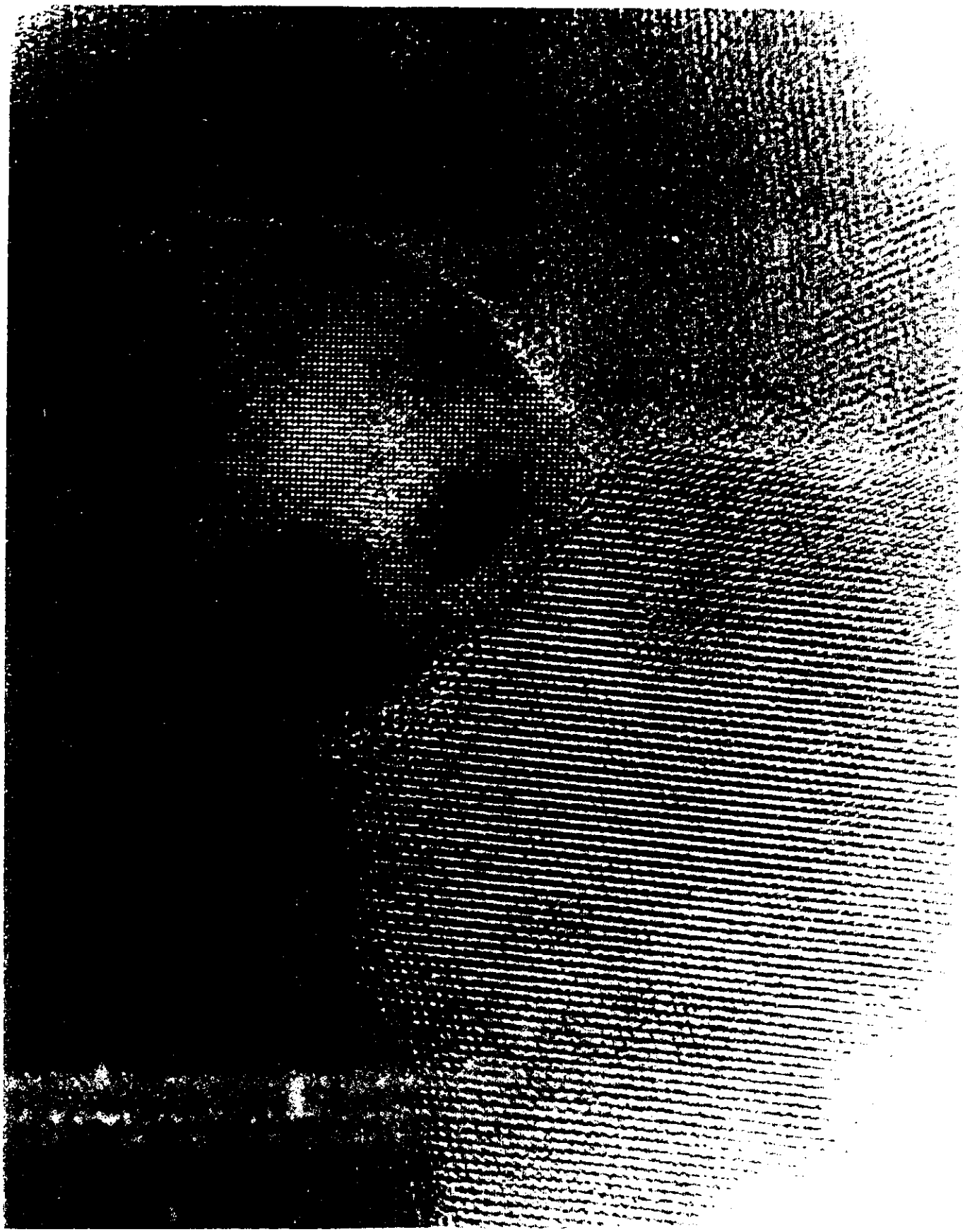

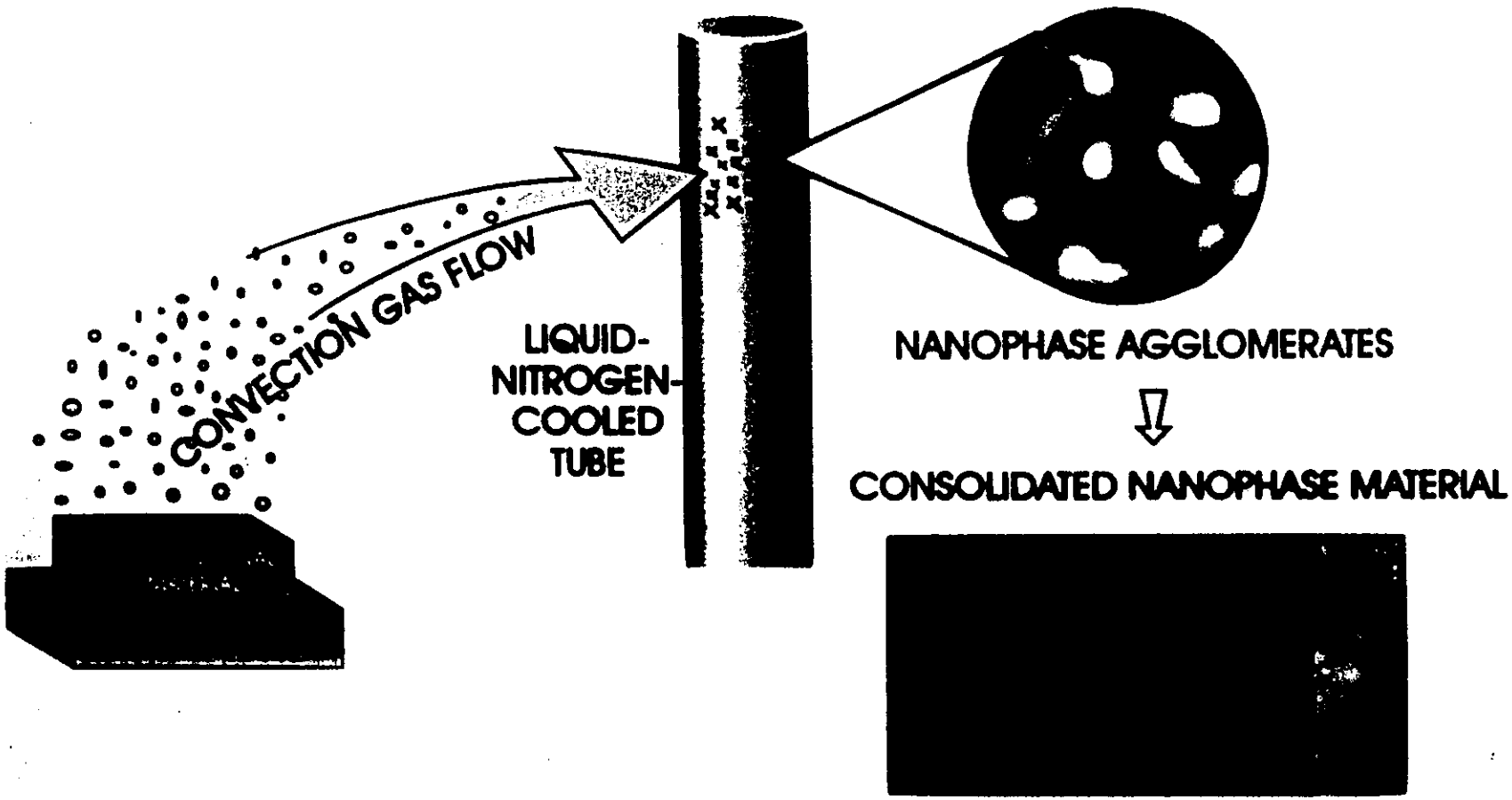
CONVECTION GAS FLOW
LIQUID-
NITROGEN-
COOLED
TUBE
NANOPHASE AGGLOMERATES
CONSOLIDATED NANOPHASE MATERIAL

What kind of information is needed?

- Crystal structure
- Chemical composition
- Shape and shape evolution
- Atomic bonds
- Orientation of the film with respect to the substrate
- Defects on the film structure

Techniques to characterize thin films and nanostructures

- Transmission electron microscopy
  - HREM, EDS, EELS, ED
- X-Ray diffraction
  - Lab source
  - High intensity source
- Microbeam X-Ray analysis
- Surface techniques
  - LEED, XPS, AUGER, etc.
- Scanning electron microscopy
  - High vacuum
  - Low vacuum
- ION Beams
  - PIXE, RBS, Nuclear Resonance, etc.
- Atomic Force Microscopy
- Scanning Tunneling Microscopy
- Atom Probe Microscopy

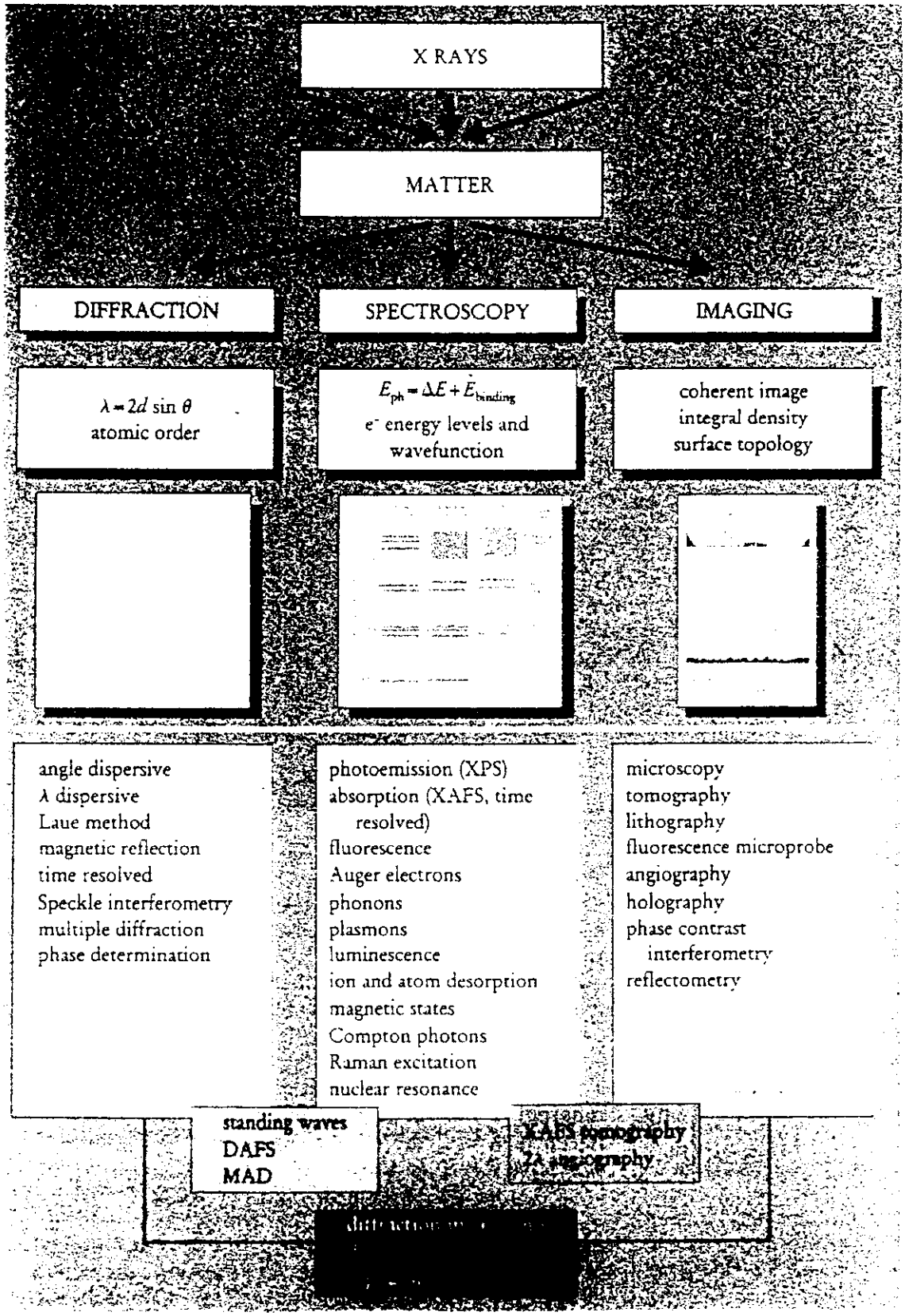
X RAYS
MATTER
DIFFRACTION
SPECTROSCOPY
IMAGING
$\lambda = 2d \sin\theta$
atomic order
$E_{ph} = \Delta E + E_{binding}$
e⁻ energy levels and wavefunction
coherent image
integral density
surface topology
angle dispersive
λ dispersive
Laue method
magnetic reflection
time resolved
Speckle interferometry
multiple diffraction
phase determination
photoemission (XPS)
absorption (XAFS, time resolved)
fluorescence
Auger electrons
phonons
plasmons
luminescence
ion and atom desorption
magnetic states
Compton photons
Raman excitation
nuclear resonance
microscopy
tomography
lithography
fluorescence microprobe
angiography
holography
phase contrast interferometry
reflectometry
standing waves
DAFS
MAD

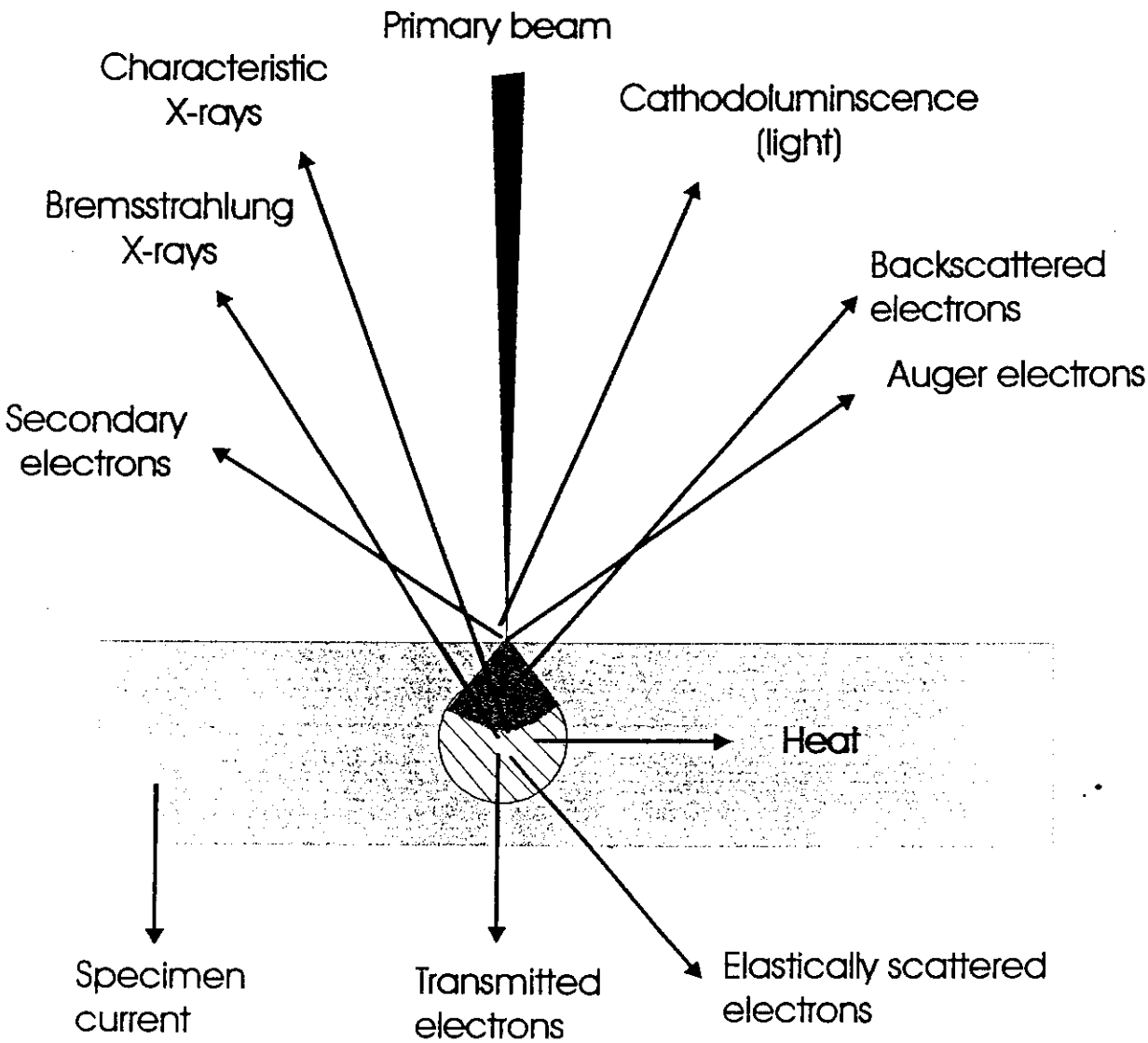
Primary beam
Characteristic X-rays
Cathodoluminscence (light)
Bremsstrahlung X-rays
Backscattered electrons
Auger electrons
Secondary electrons
Heat
Specimen current
Transmitted electrons
Elastically scattered electrons

ININ

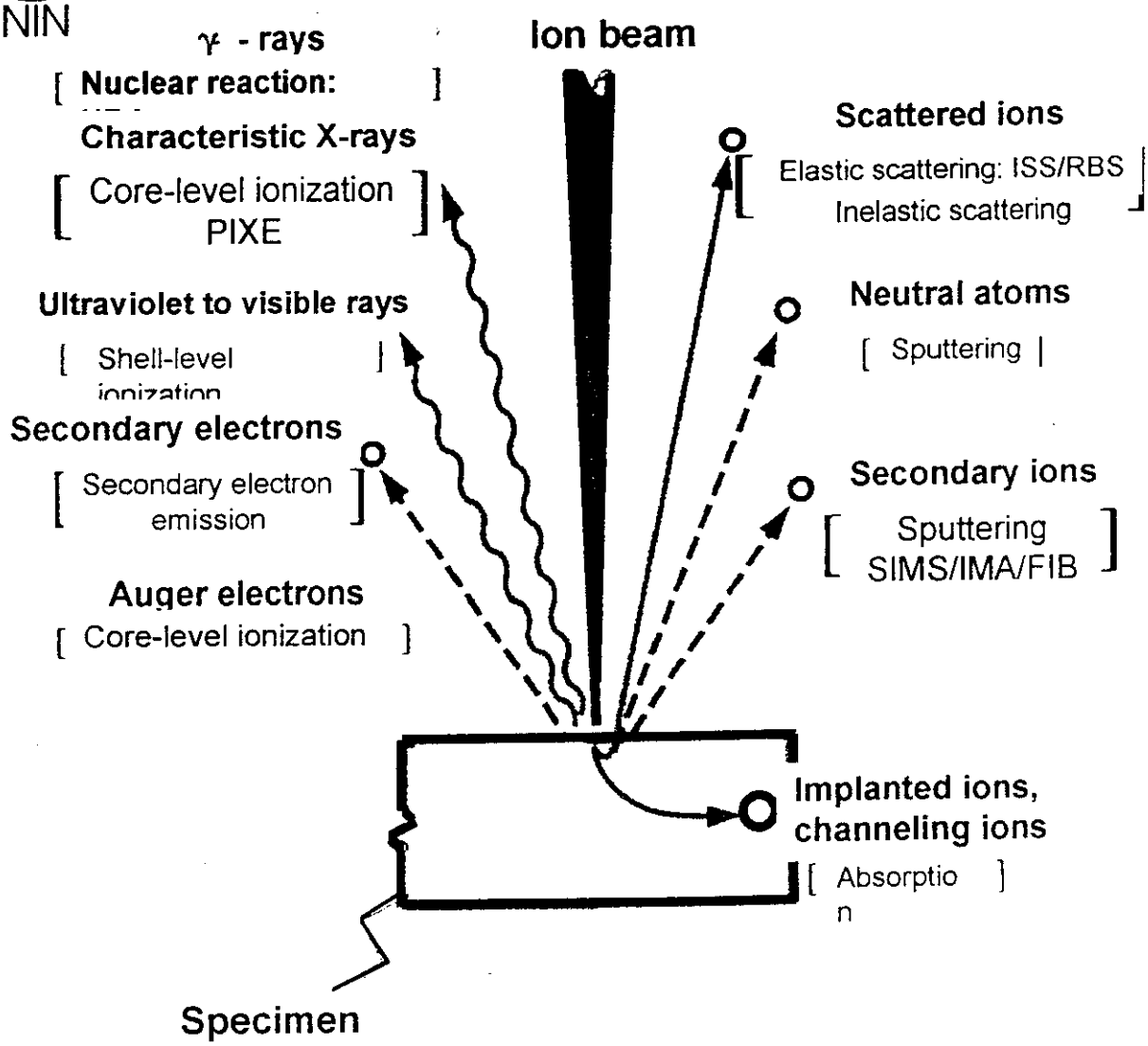

<Acronym>	<Instrumental Method>
NRA	Nuclear reaction analysis
PIXE	Particle induce X-ray emission spectroscopy
ISS	Ion scattering spectroscopy
RBS	Rutherford backscattering spectroscopy
FIB	Focused ion beam technology
SIMS	Secondary ion mass spectroscopy
IMA (IMMA)	Ion micro-mass analysis

External view of JEM-2010F

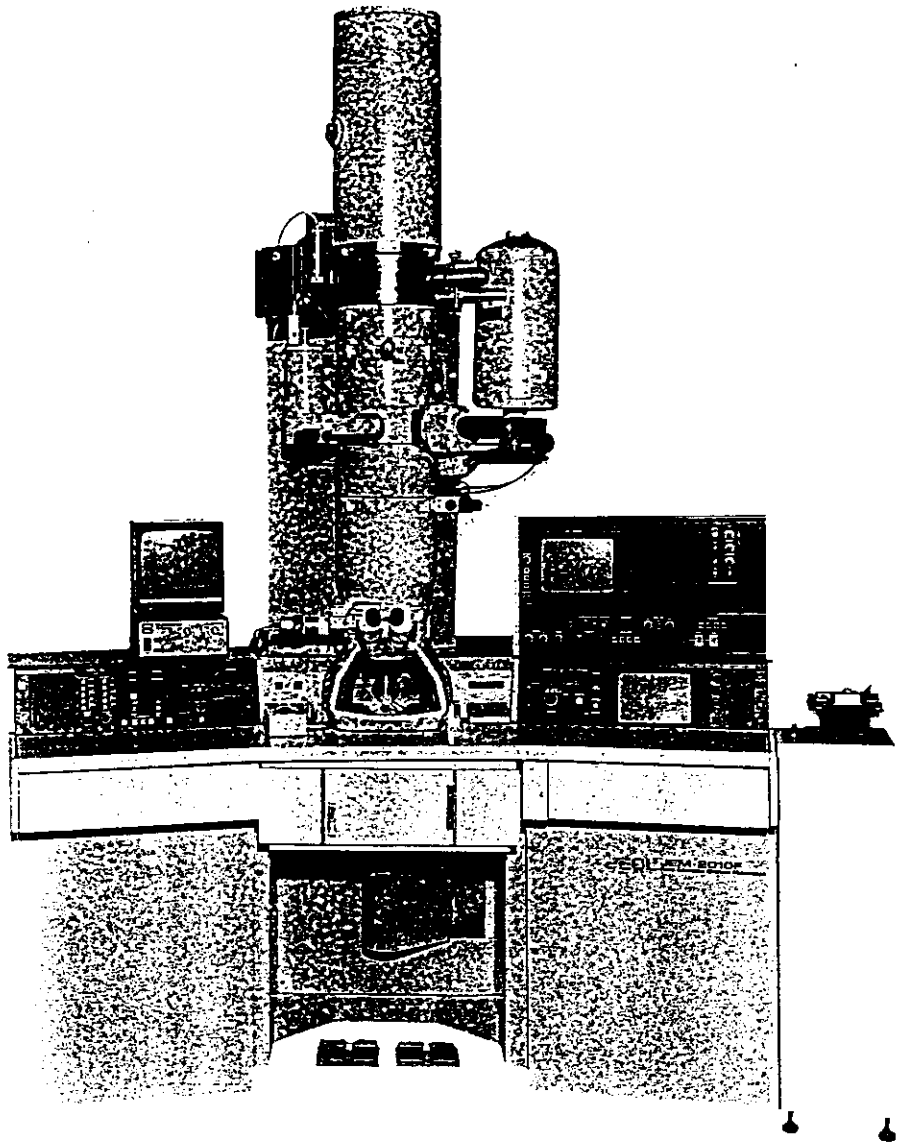

Field emission high-resolution analytical electron microscope, JEM-2010F

Shown above is the external view of the JEM-2010F. The instrument can be equipped with optional energy dispersive X-ray spectrometers (EDS), a parallel detection electron energy loss spectrometer (PEELS), a scanning image observation device (ASID), and TV units including one to be installed simultaneously with PEELS.

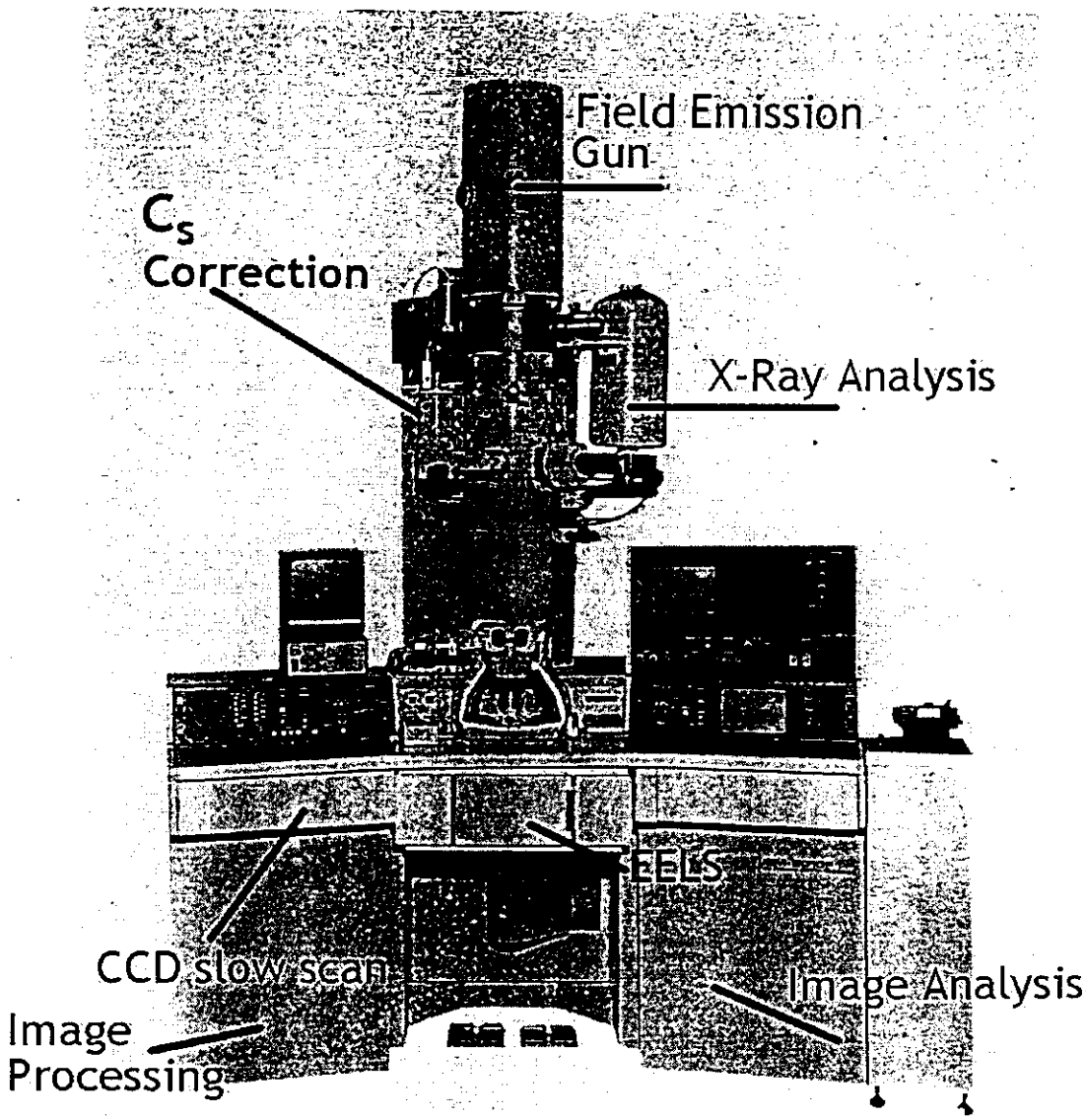

Field emission high-resolution analytical electron microscope, JEM-20100F

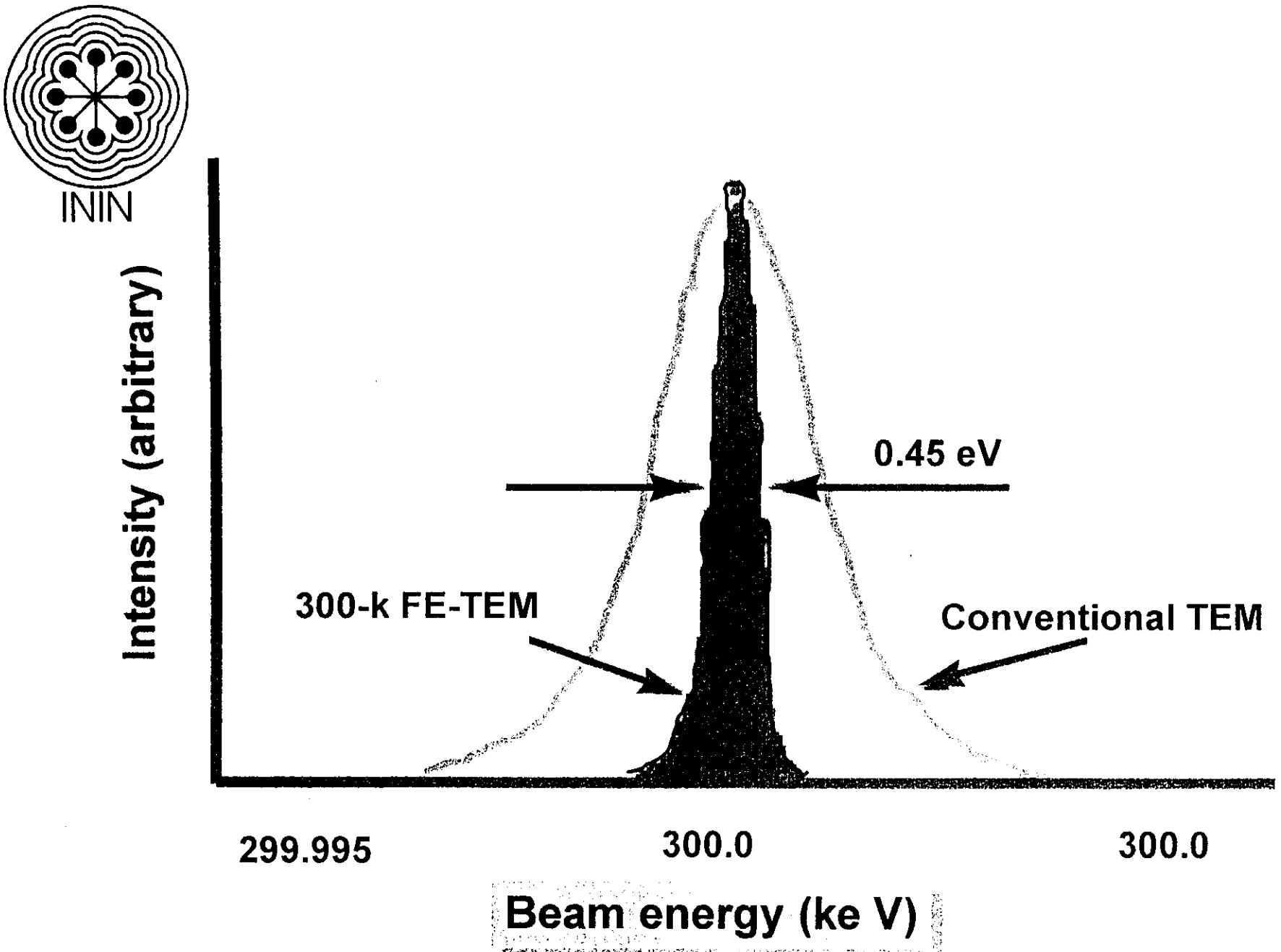
ININ
Intensity (arbitrary)
0.45 eV
300-k FE-TEM
Conventional TEM
299.995
300.0
300.0
Beam energy (ke V)

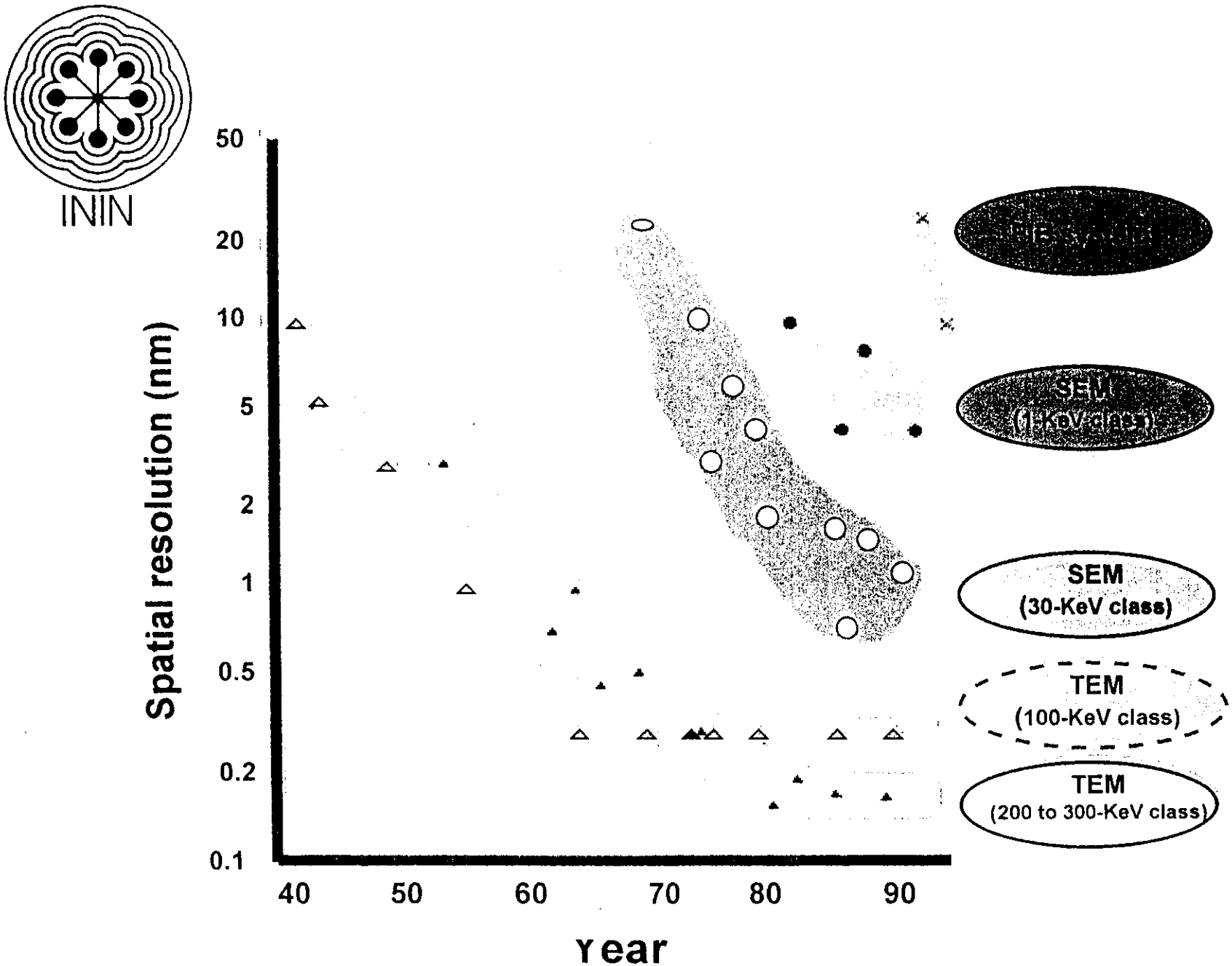
ININ
Spatial resolution (nm)
50
20
10
5
2
1
0.5
0.2
0.1
40
50
60
70
80
90
Year
SEM
(1-KeV class)
SEM
(30-KeV class)
TEM
(100-KeV class)
TEM
(200 to 300-KeV class)

Specimen Preparation

- Sample has to be as thin as possible so the elastic scattering will dominate
- Mechanical stability
- Clean sample
- Sample without substrate
- Usually thin so can be mounted on a proper grid. If necessary ion-milling or electropolishing.
- Sample with the substrate.

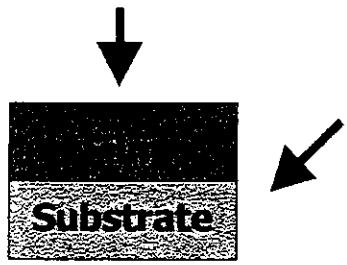

Initial thinning
Mechanical punch
Ion milling
Chemical polishing

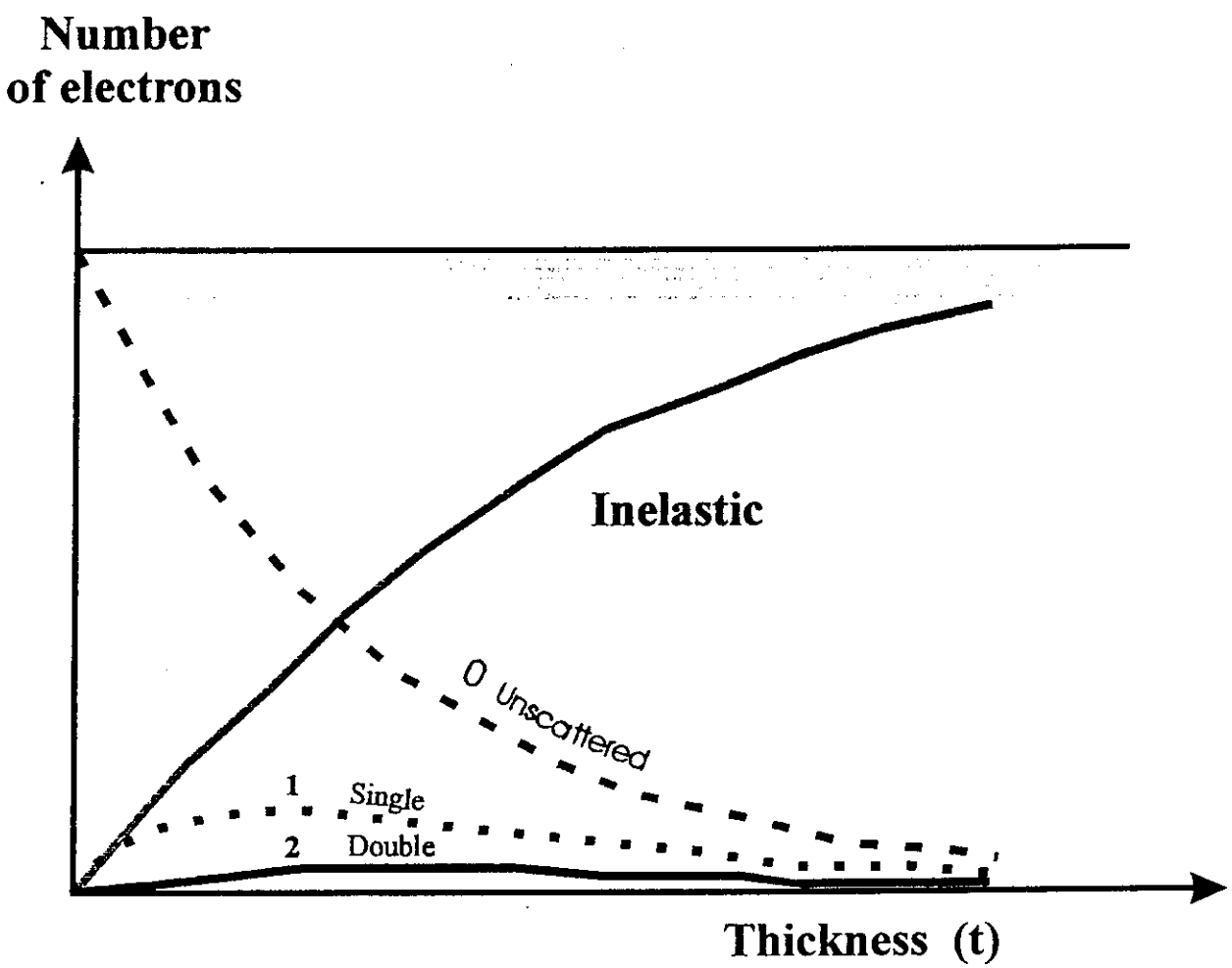
Number
of electrons
Inelastic
0 Unscattered
1 Single
2 Double
Thickness (t)

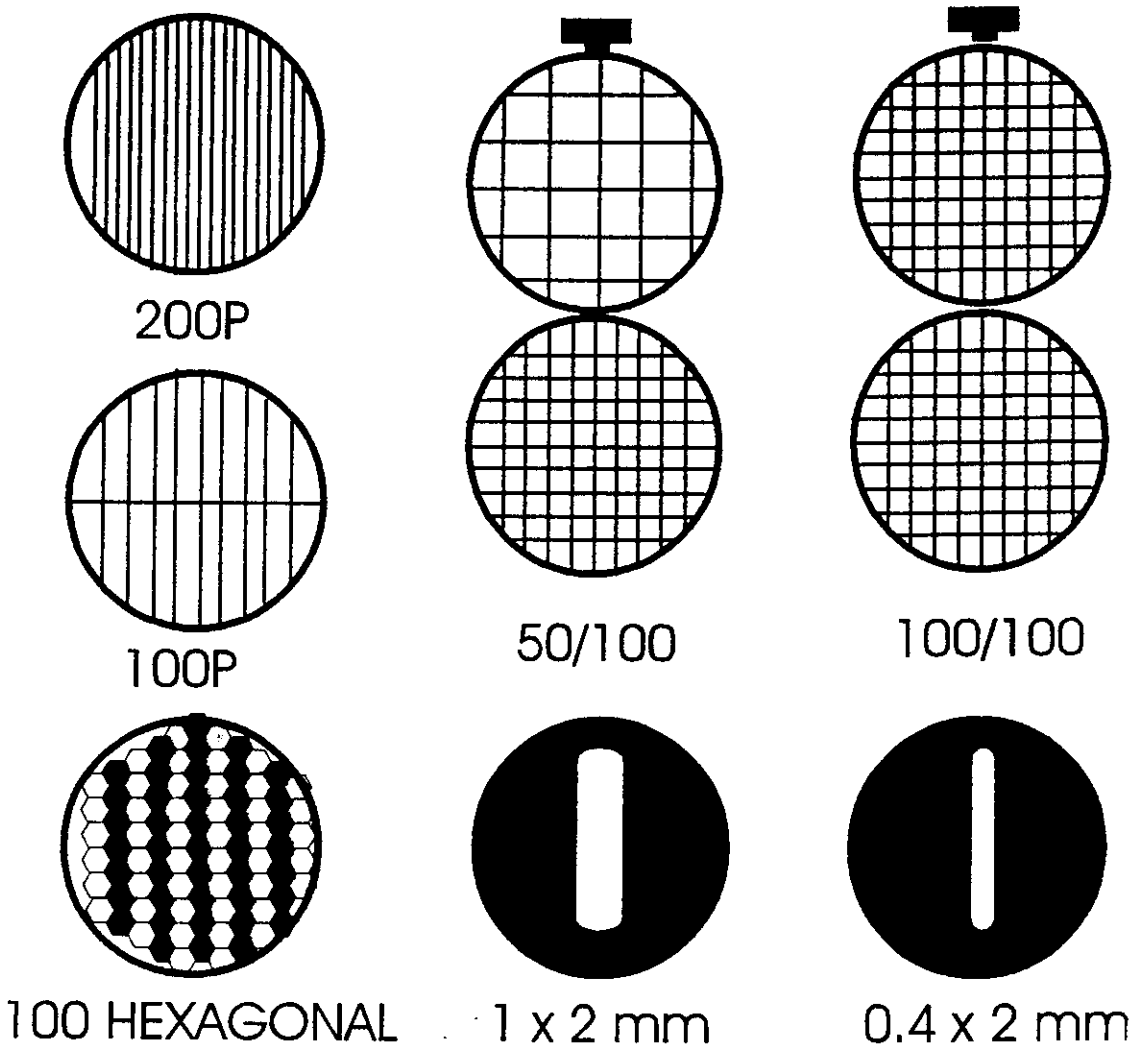

A variety of specimen support grids of different mesh size and shape. At the top right is the oyster grid, useful for sandwiching small slivers of thin material.

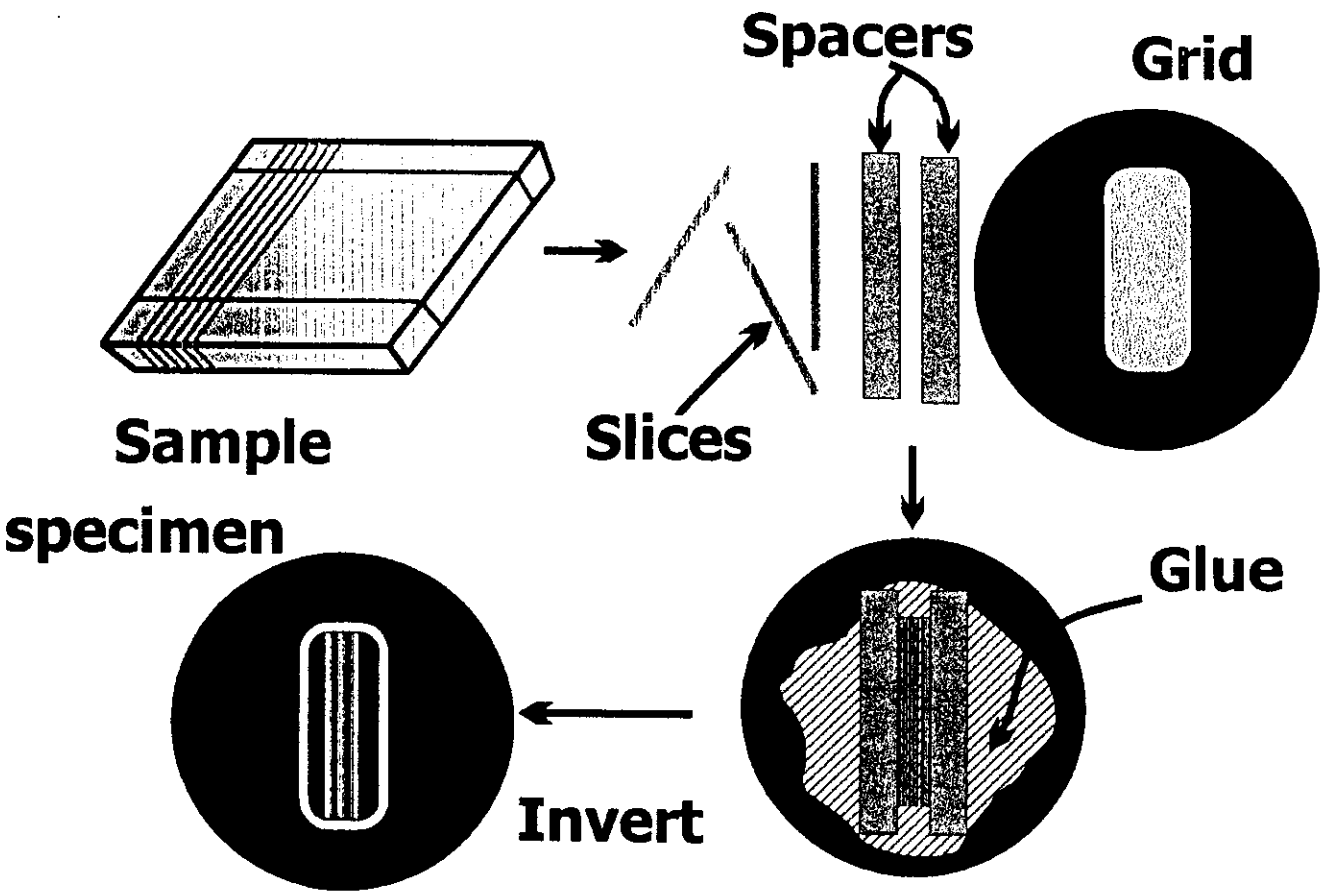

Schematic sequence for cross-section specimen preparation; the sample is cut into slices normal to the interfaces which are glued together between spacers which could be Si, glass, or some other inexpensive material so that they are wider tha the slot in the grid. The "club" sandwich is then itself glued to the grid (over the slot) and ion milled to perforation.

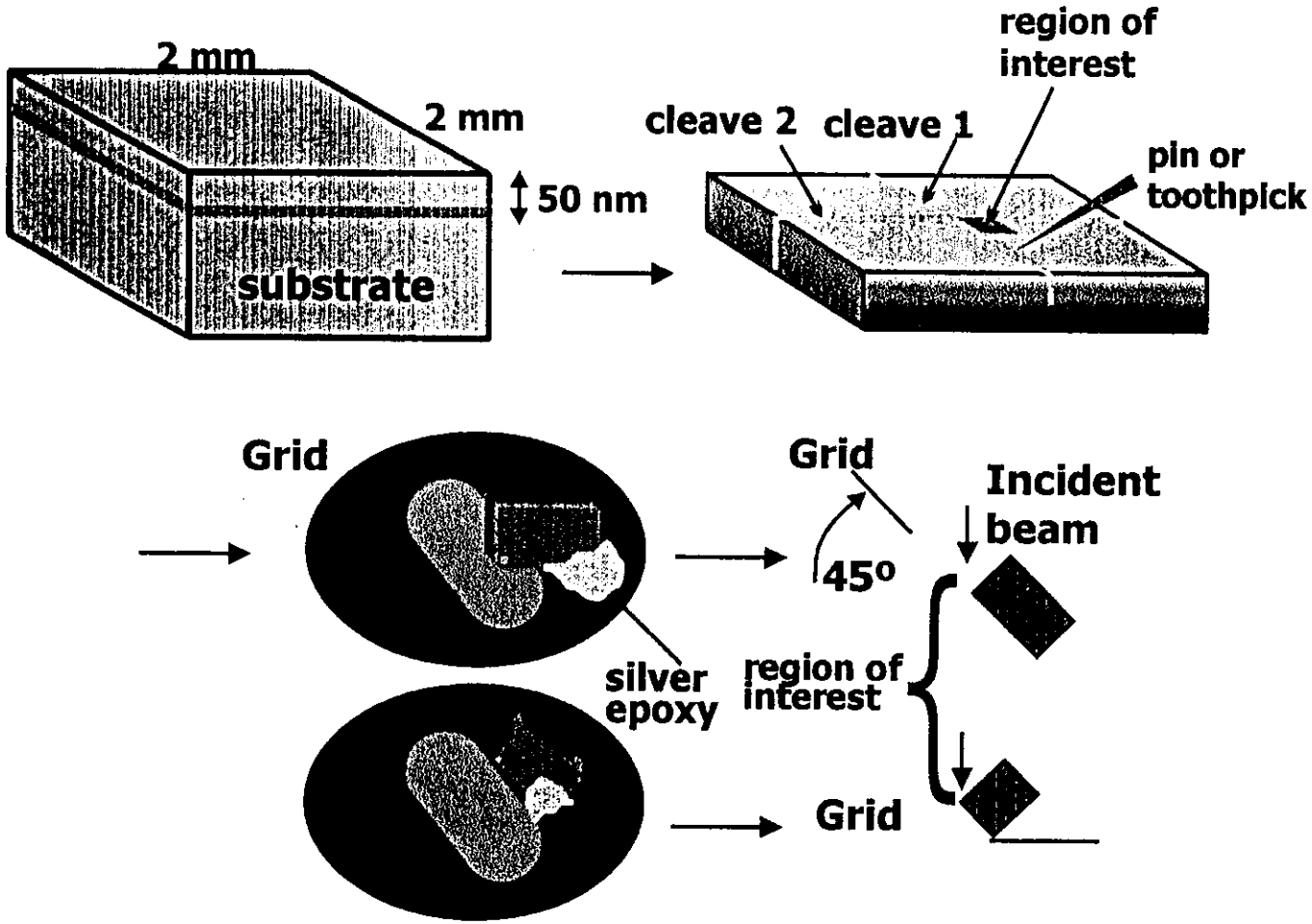

The 90°-wedge specimen: prethin to create a 2-mm saqure of the multilayers on a Si substrate; scribe the Si through the surface layers, turn over, and cleave; inspect to make sure the cleavage is clean; giving a sharp 90° edge; reject of not; mount the 90° corner over the edge of a hole in a Cu grid, then insert in the TEM; note that two different orientations are available from a single cleavage operation.

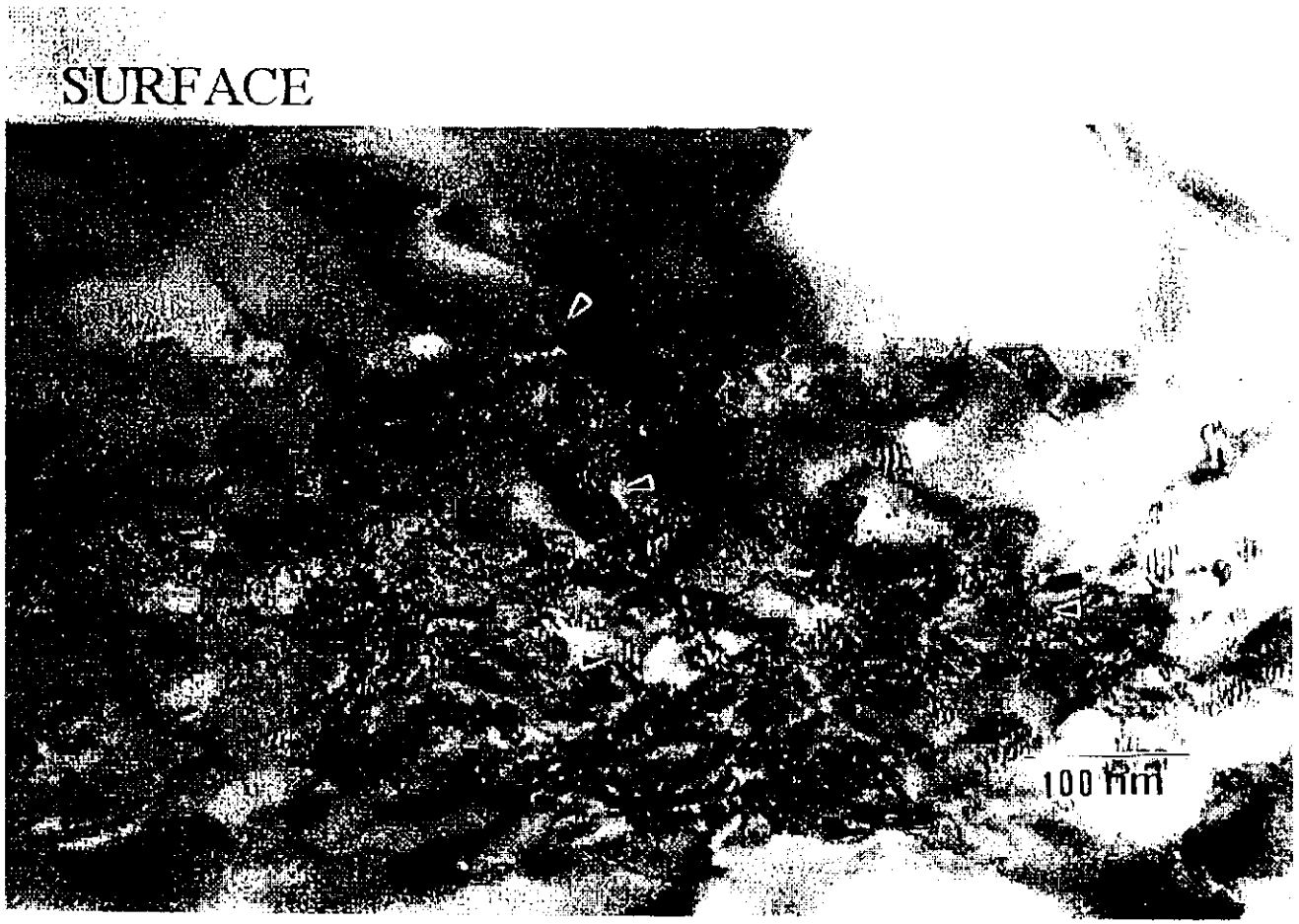
SURFACE
100 nm

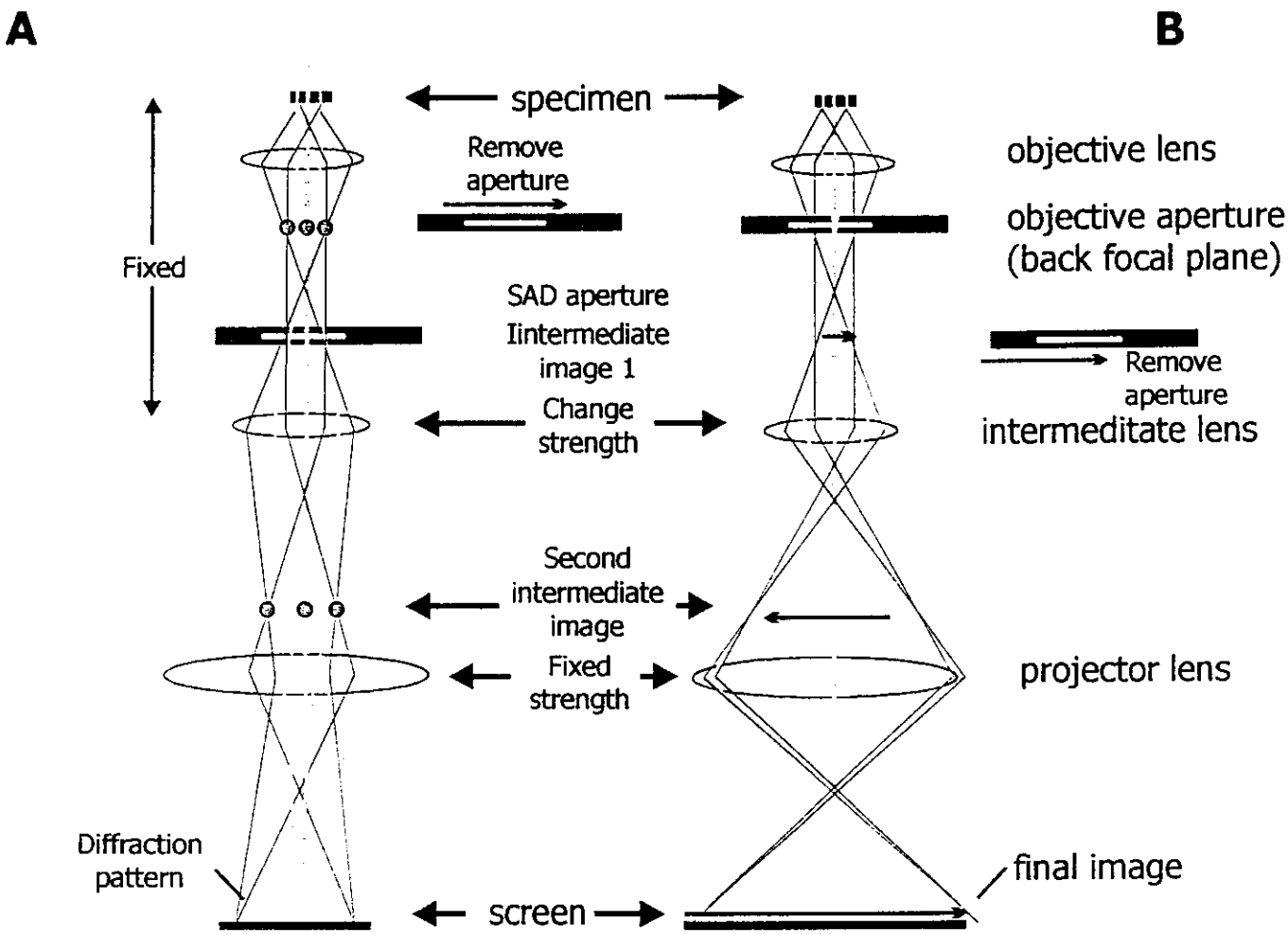

The two basic operations of the TEM imaging system involve (A) projecting the diffraction pattern on the viewing screen and (B) projecting the image onto the screen. In each case the intermediate lens selects either the back focal plane or the image plane of the objective lens as its object.

Electron Diffraction

The formation of an electron diffraction pattern from a thin crystal. The diffraction pattern is a projection of the reciprocal lattice section in the plane of the crystal normal to the electron beam. The beam divergences are greatly exaggerated.

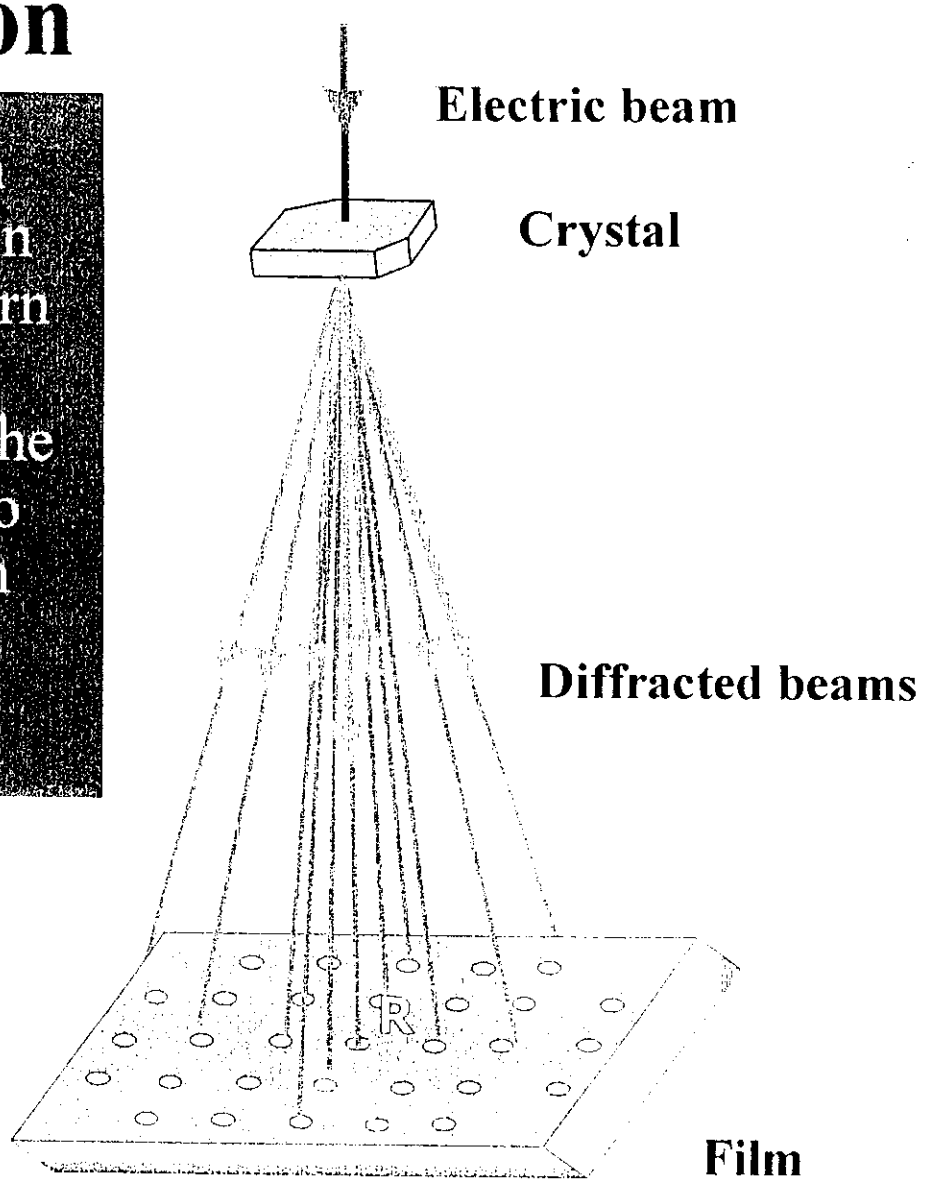

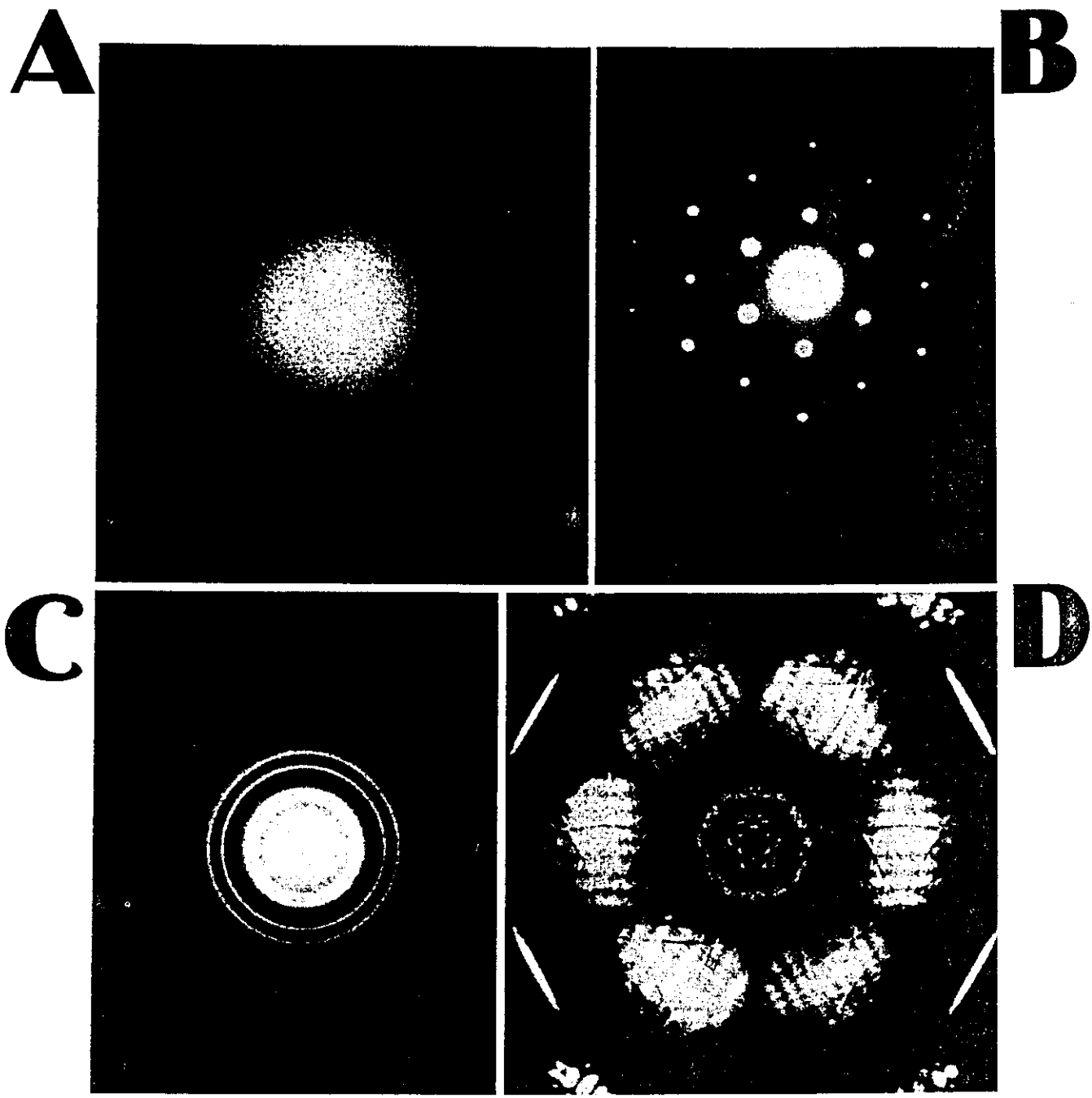

Several kinds of diffraction patterns obtained from a range of materials in a conventional 100 kV TEM: (A) amorphous carbon, (B) an Al single crystal, (C) polycrystalline Au, (D) Si illuminated with a convergent beam of electrons. In all cases the direct beam of electrons is responsible for a bright intensity at the center of the pattern and the scattered beams account for the spots or rings that appear around the direct beam.

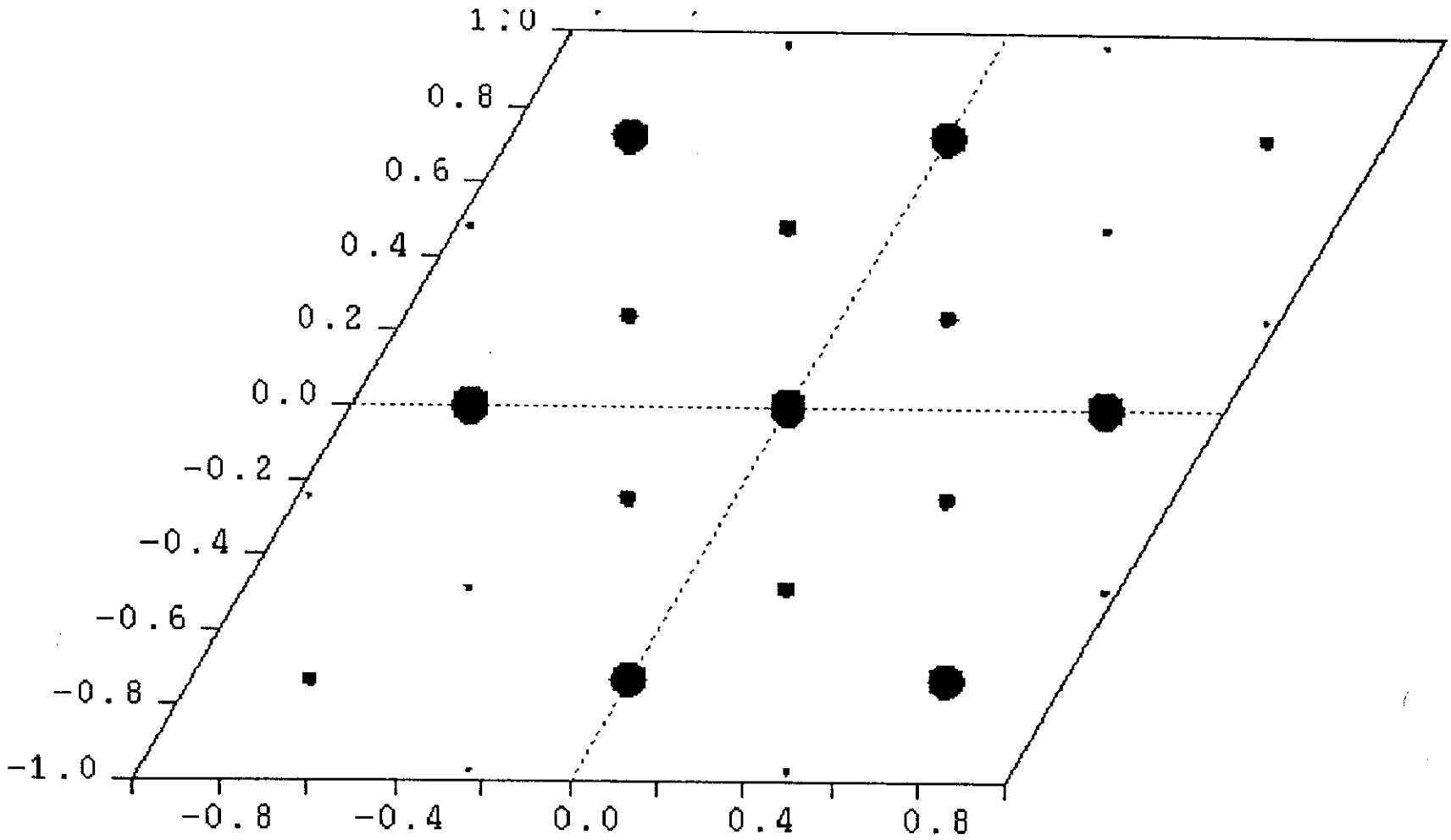

Al001

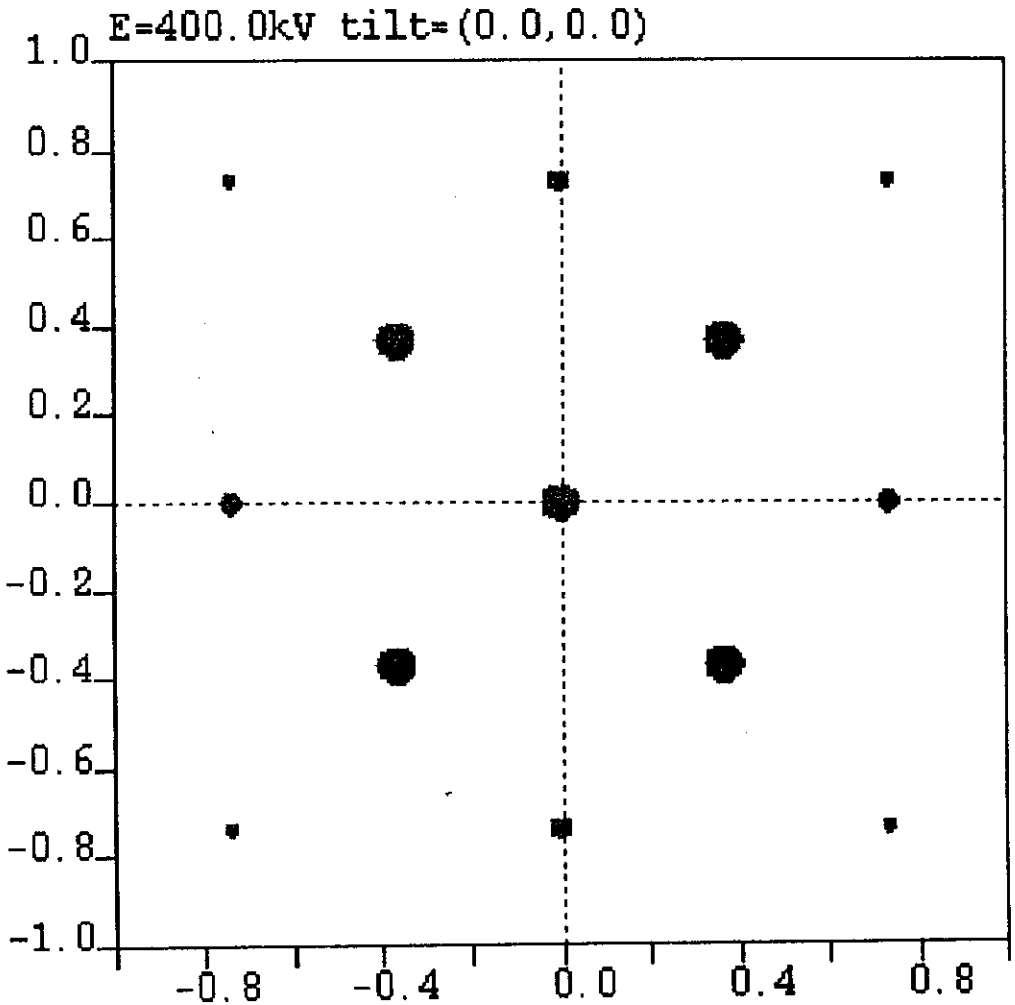

Si001

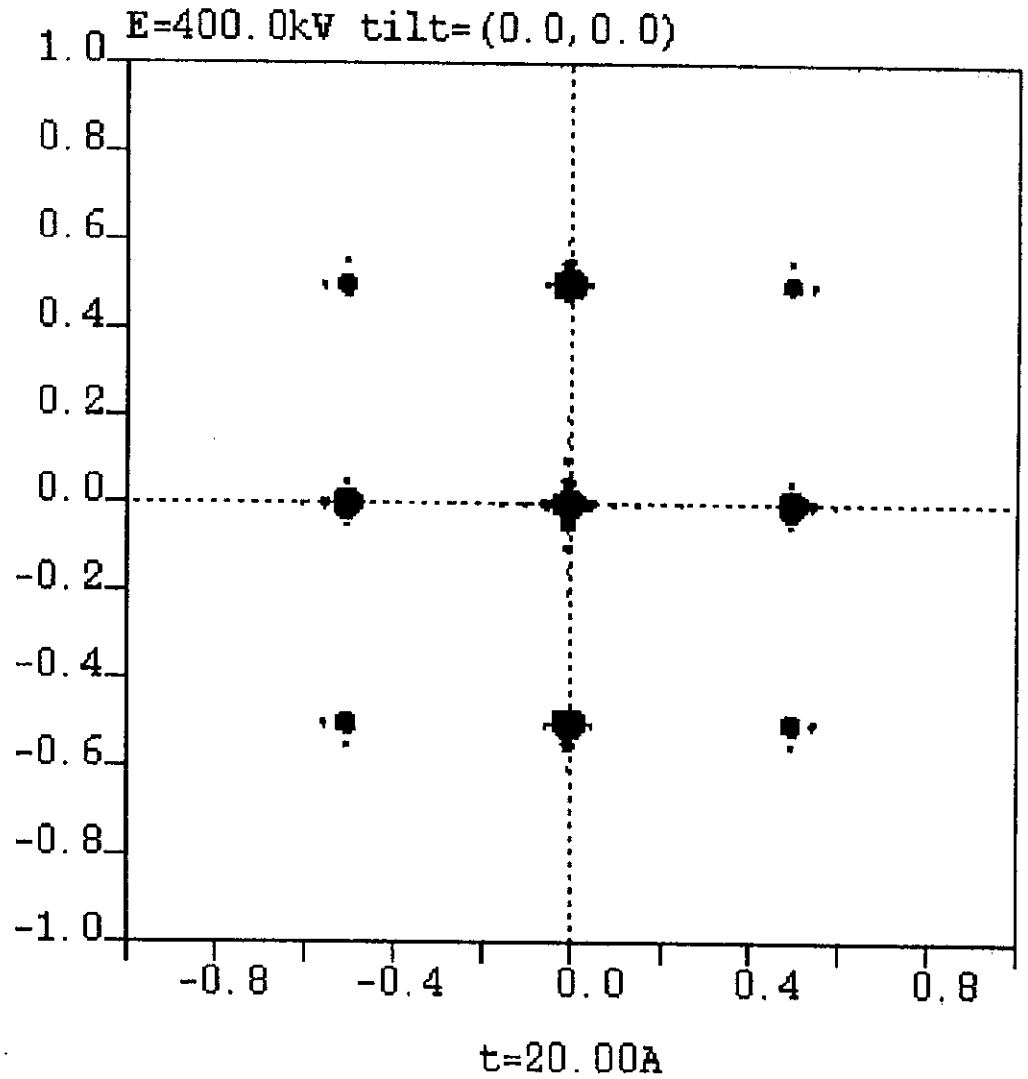
E=400.0kV tilt=(0.0,0.0)
1.0
0.8
0.6
0.4
0.2
0.0
-0.2
-0.4
-0.6
-0.8
-1.0
-0.8
-0.4
0.0
0.4
0.8
t=20.00A

Pt001

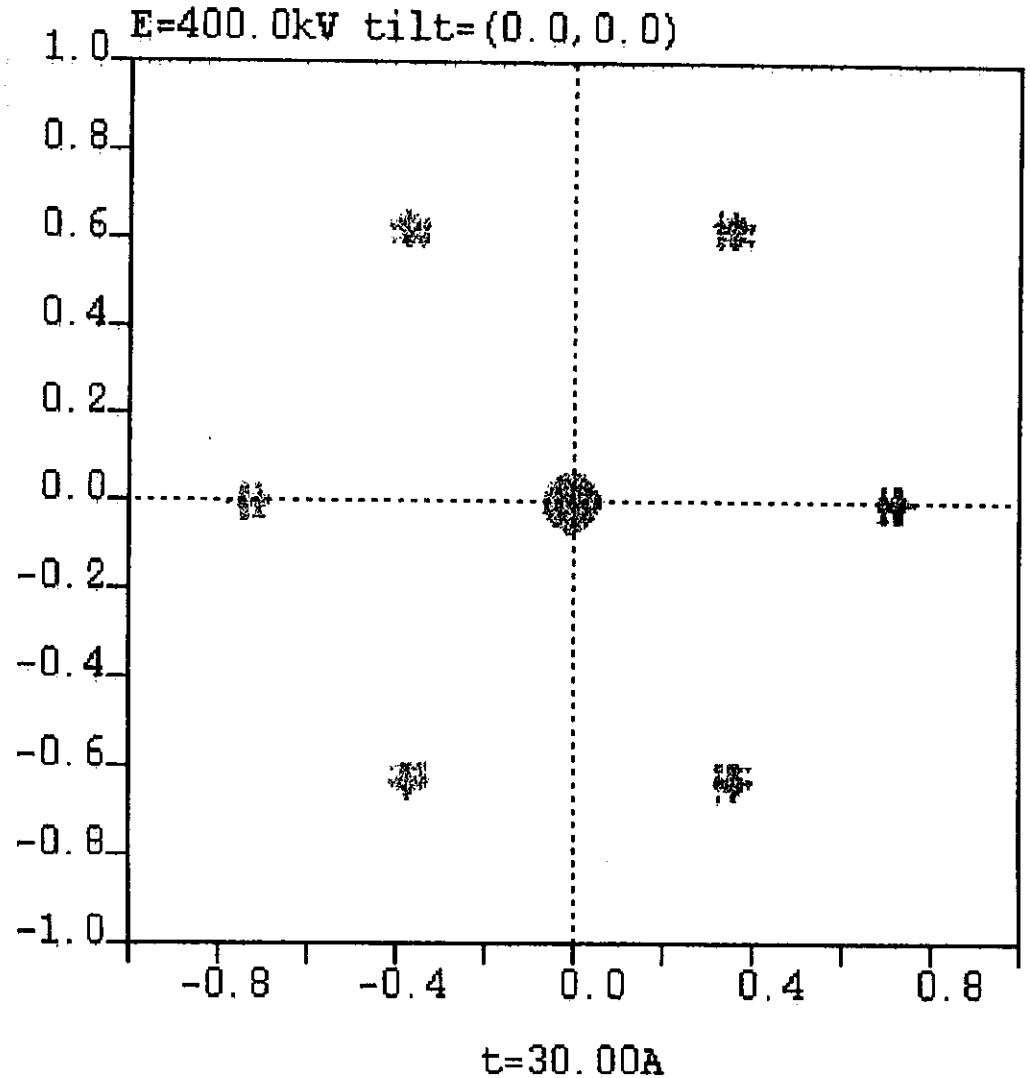
E=400.0kV tilt=(0.0,0.0)
1.0
0.8
0.6
0.4
0.2
0.0
-0.2
-0.4
-0.6
-0.8
-1.0
-0.8
-0.4
0.0
0.4
0.8
t=30.00A

Pt111

FFT's of individual Platinum particles

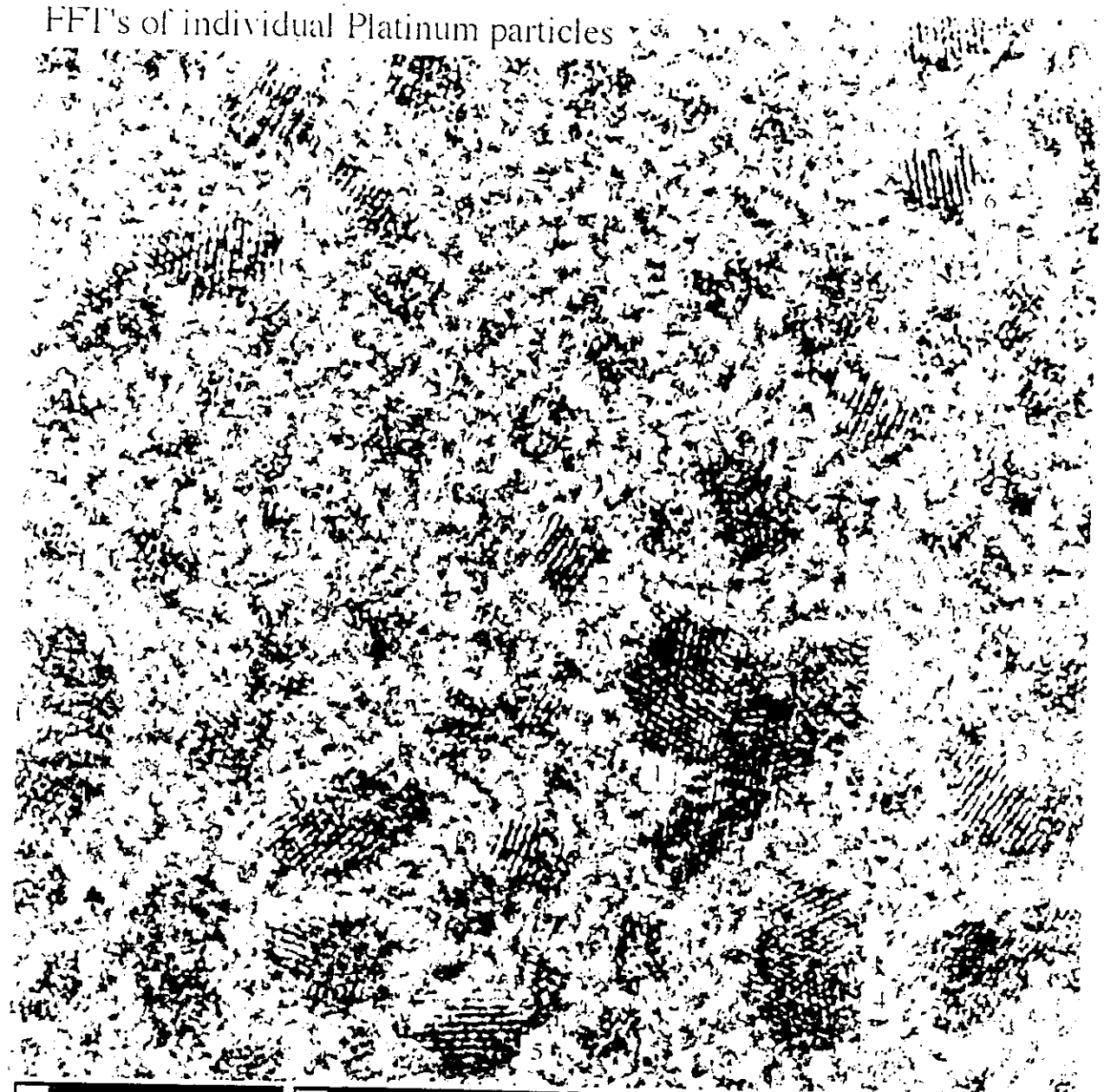

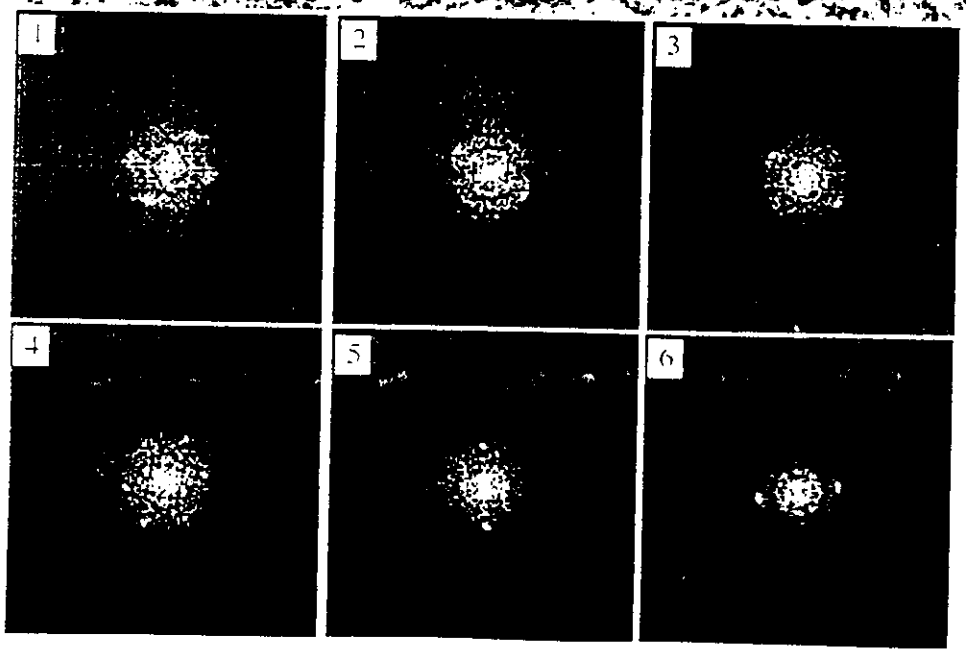

FFTSPLIT

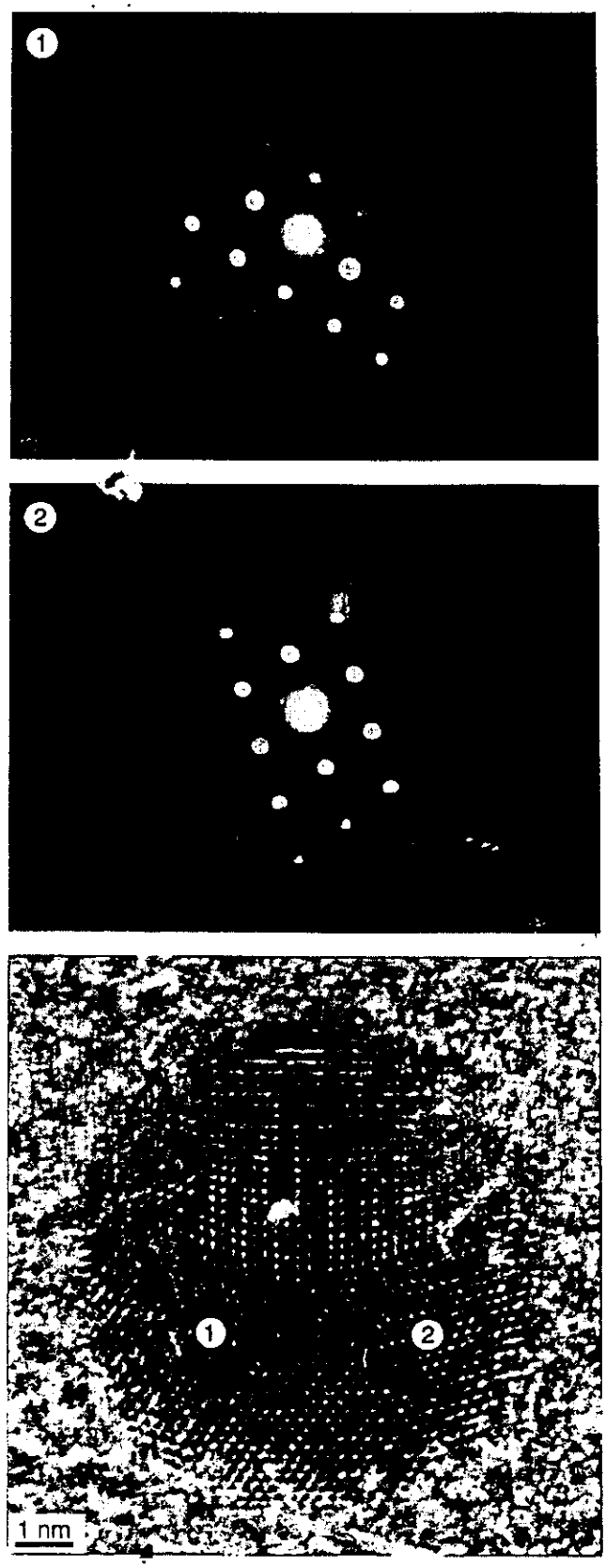
1
2
1
2
1 nm

stn 30/VI/94 #wk2108(x800) wau9.tif

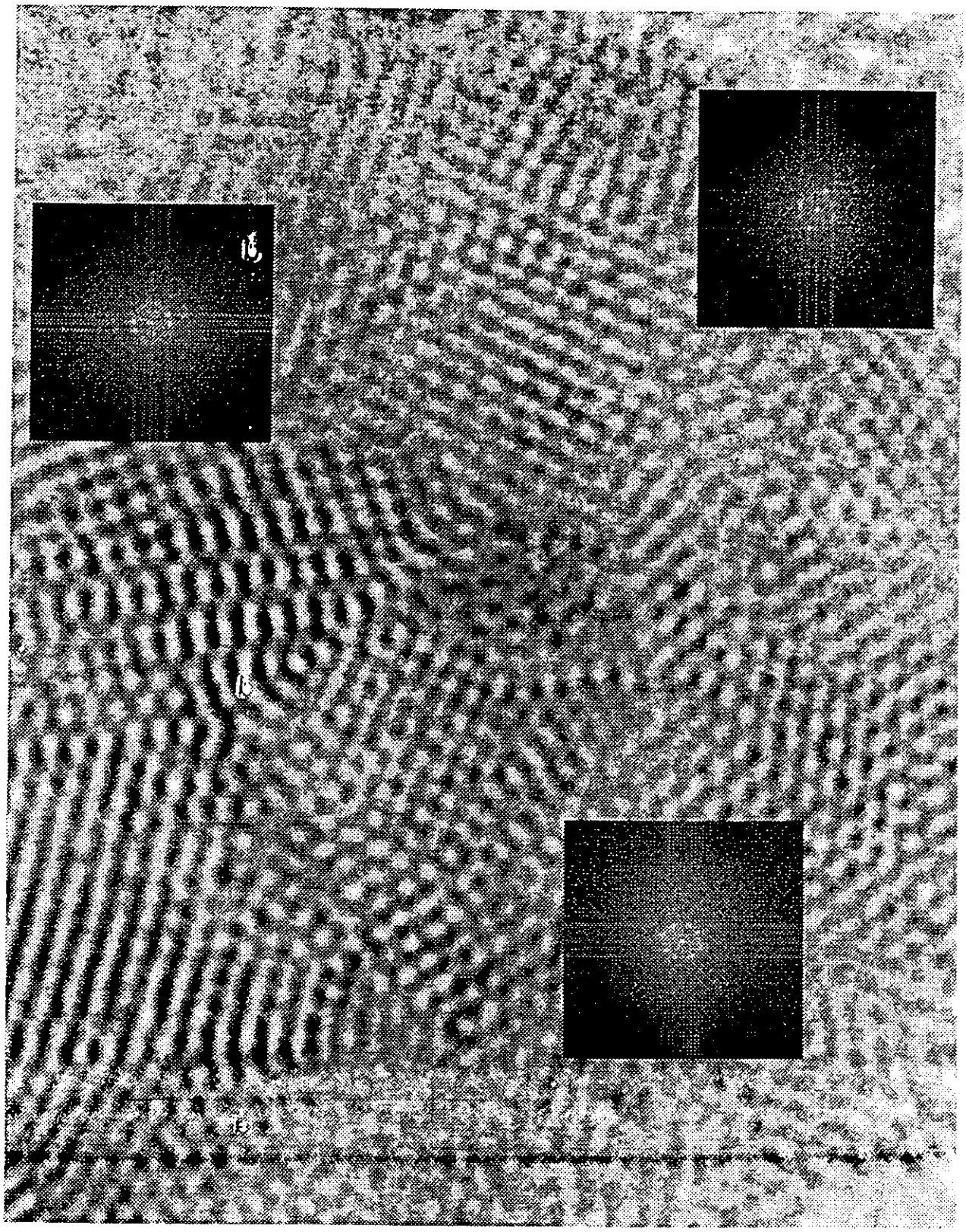

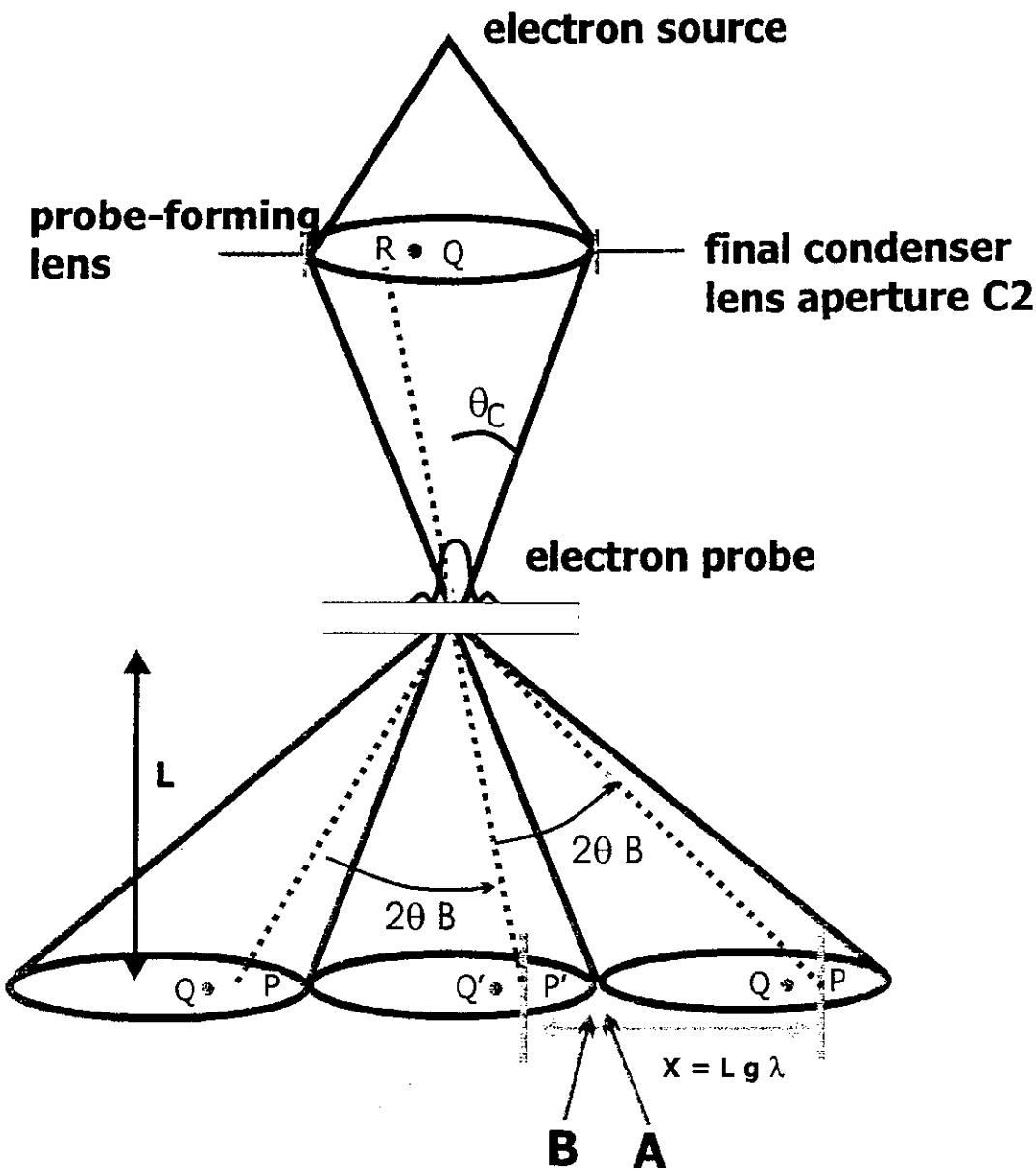

Schematic diagram of convergent beam electron diffraction. Source point P gives a set of points P′ in each disk differing by lattice vectors, point Q defines a different beam direction and a set of diffracted beams. The camera length is L.

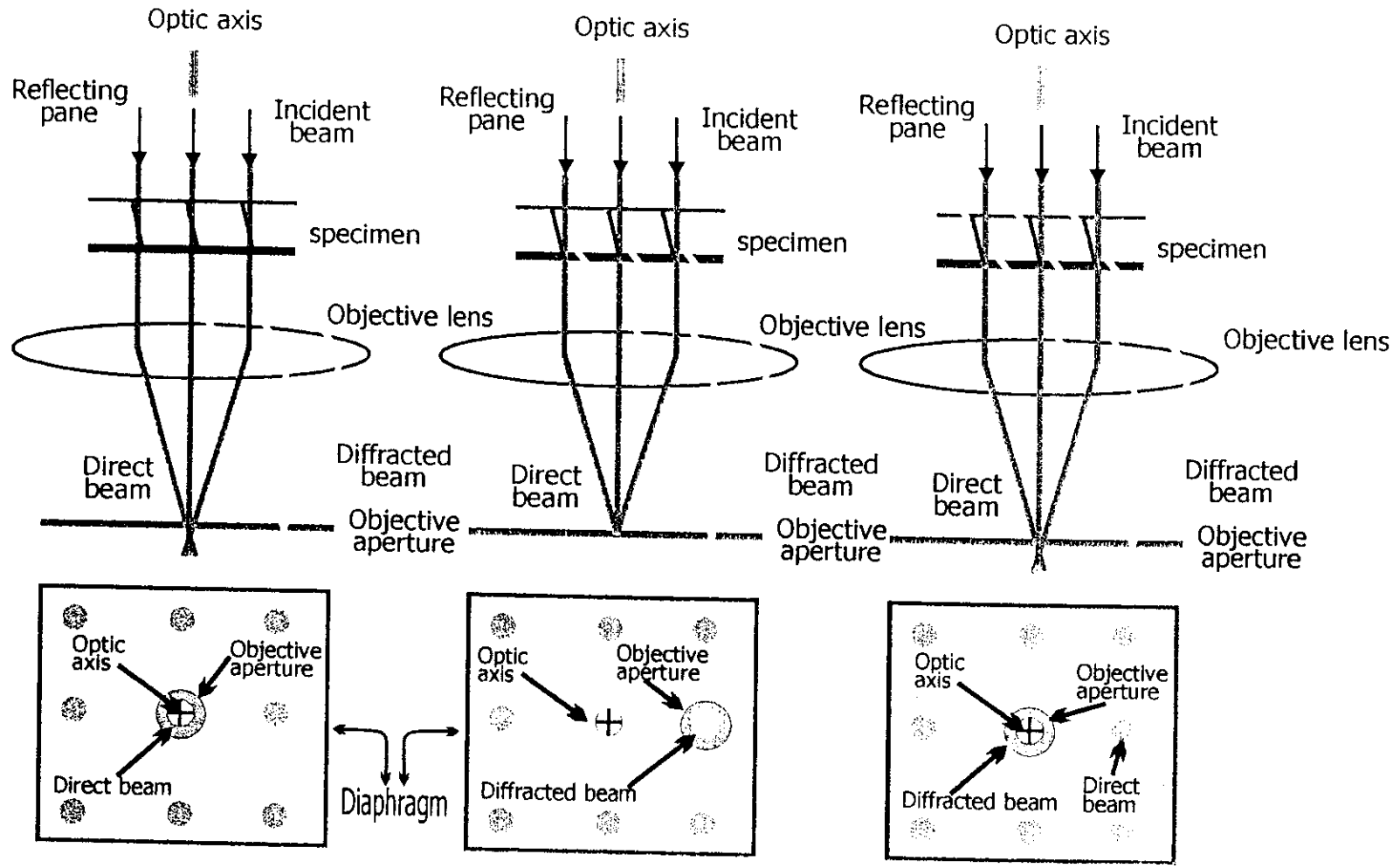

Ray diagram showing how the objective lens/aperture are used in combination to produce (A) a BF image formed from the direct beam, (B) a displaced-aperture DF image formed with a specific off-axis scattered beam, and (C) a CDF image where the incident beam is tilted so that the scattered beam remains on axis. The area selected by the objective aperture, as seen on the viewing screen, is shown below each ray diagram.

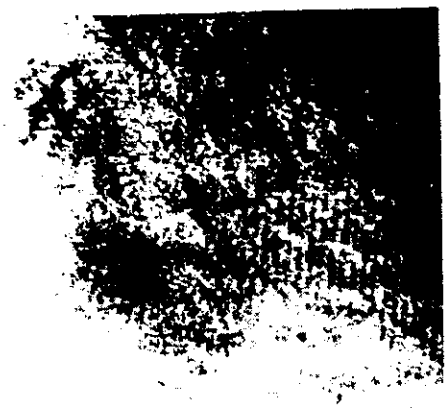

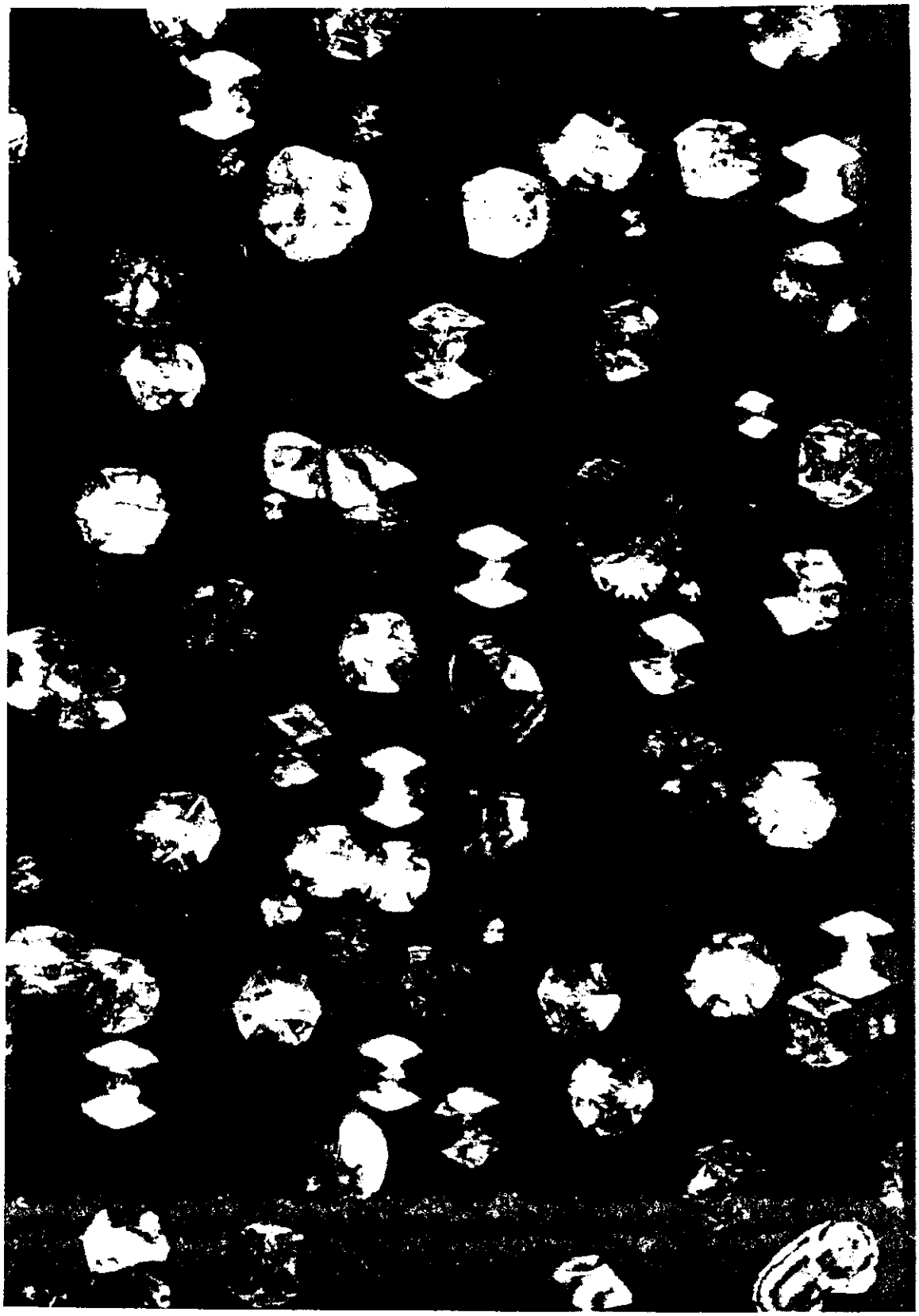

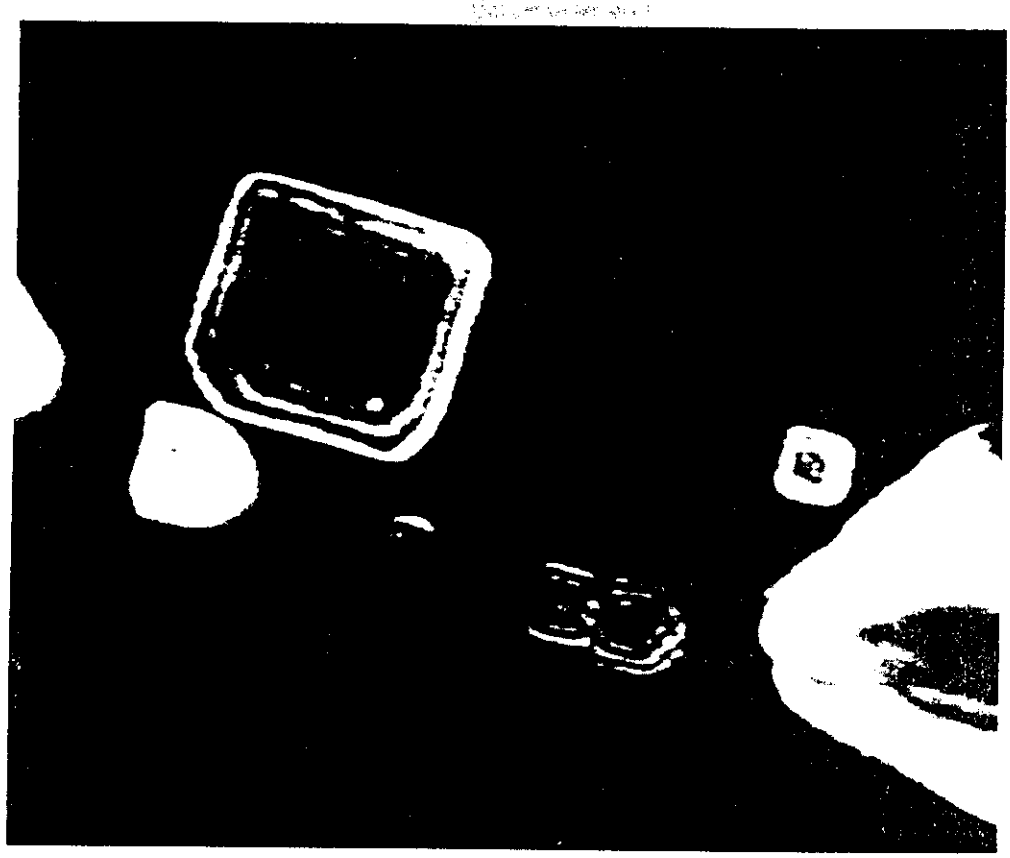

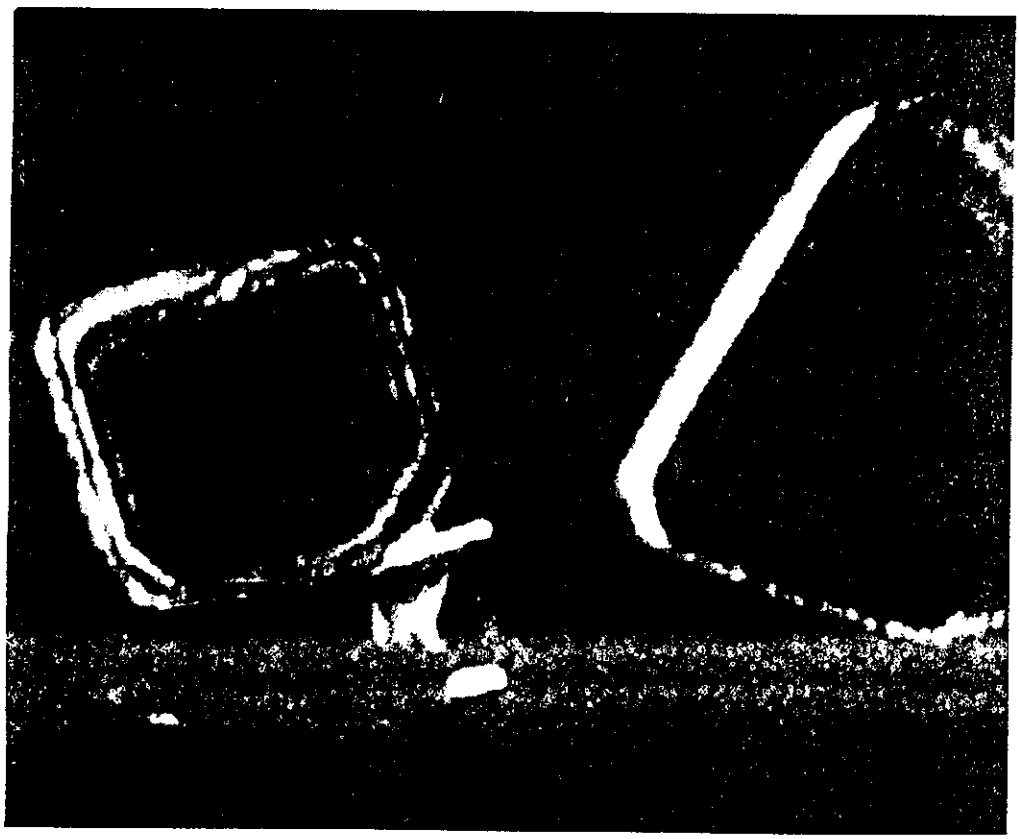

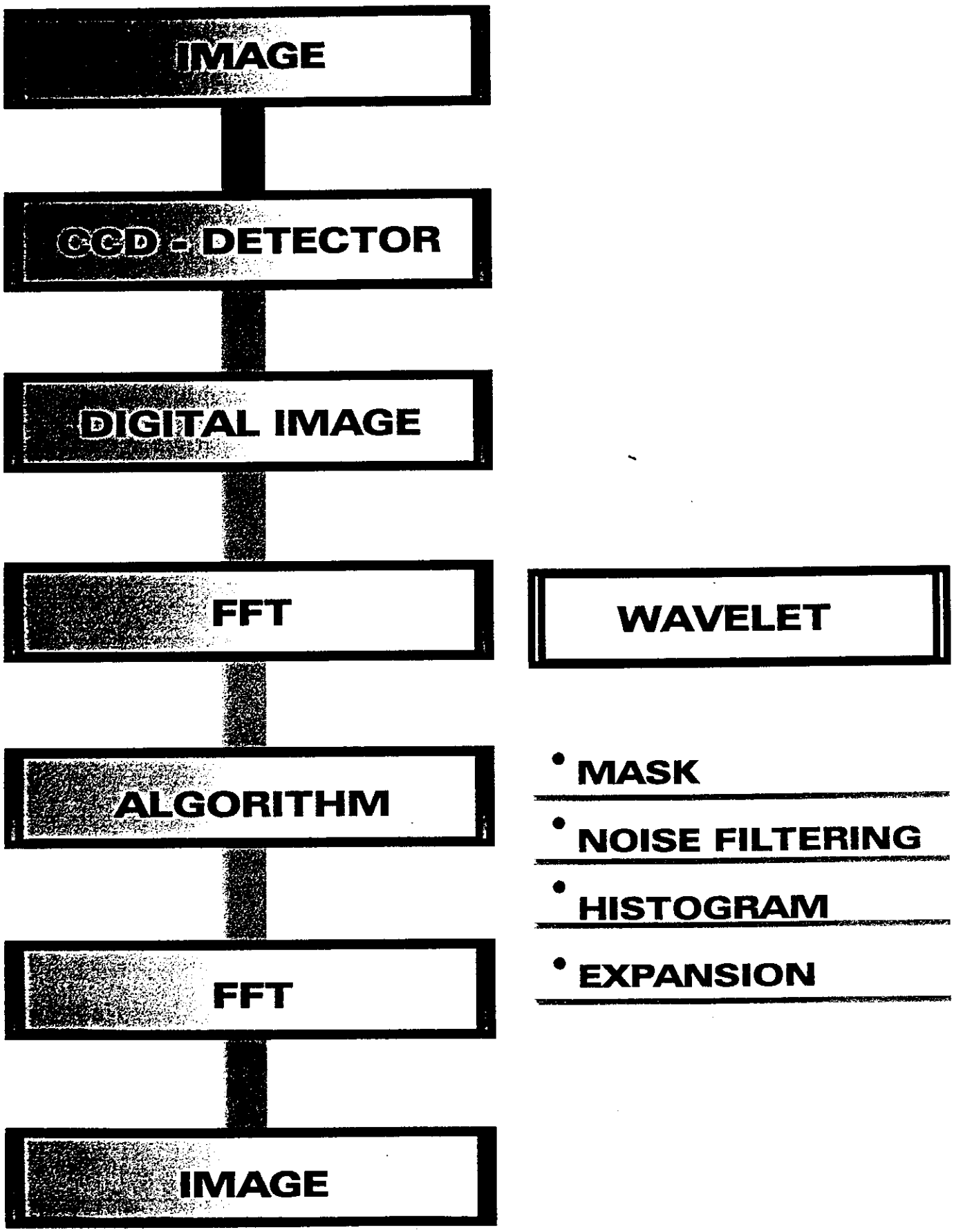
IMAGE
CCD - DETECTOR
DIGITAL IMAGE
FFT
WAVELET
ALGORITHM
• MASK
• NOISE FILTERING
• HISTOGRAM
• EXPANSION
FFT
IMAGE

BRAGG FILTERS

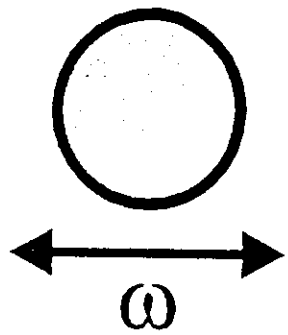

FOR AN IMAGE OF PERIOD X

W (OPTIMUN) = 0.75 1/x

PROBLEM - SUBSTRATE - PARTICLE

INTERFACE NOT WELL DEFINED

RING FILTERS

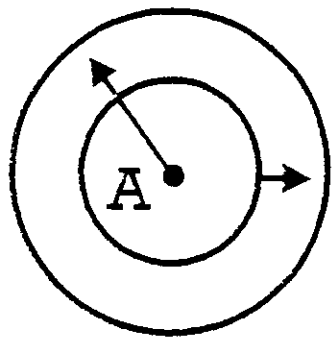

W IS THE MOST IMPORTANT PARAMETER

W → SMALL SUPPORT CONTRAST

W → LARGE NOISE SUBTRATE

W (OPTIMUN) ~ 0.5 1/X

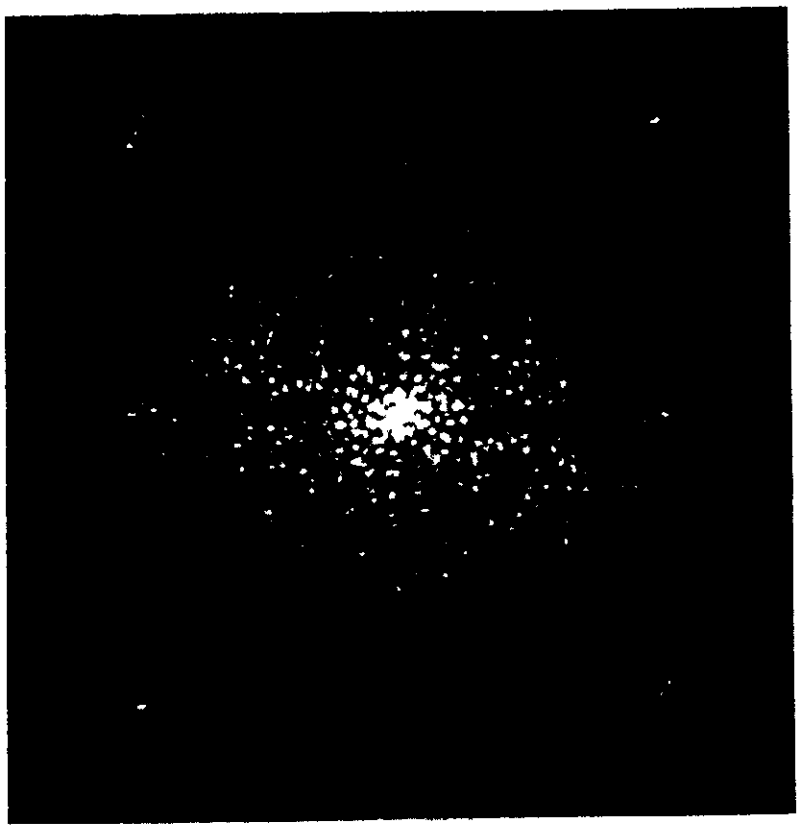

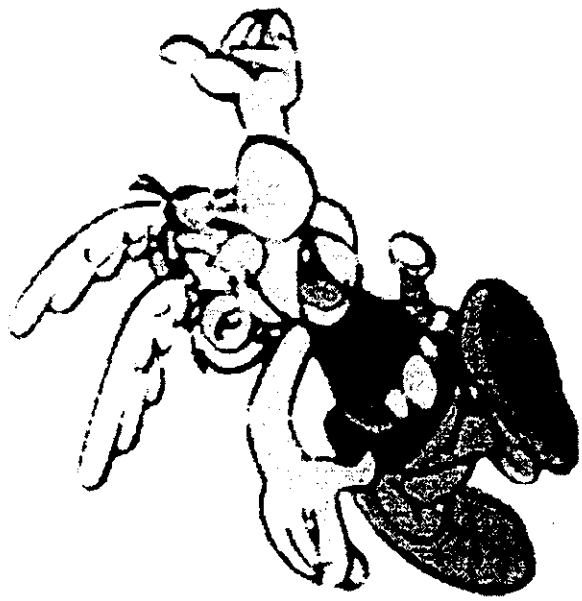

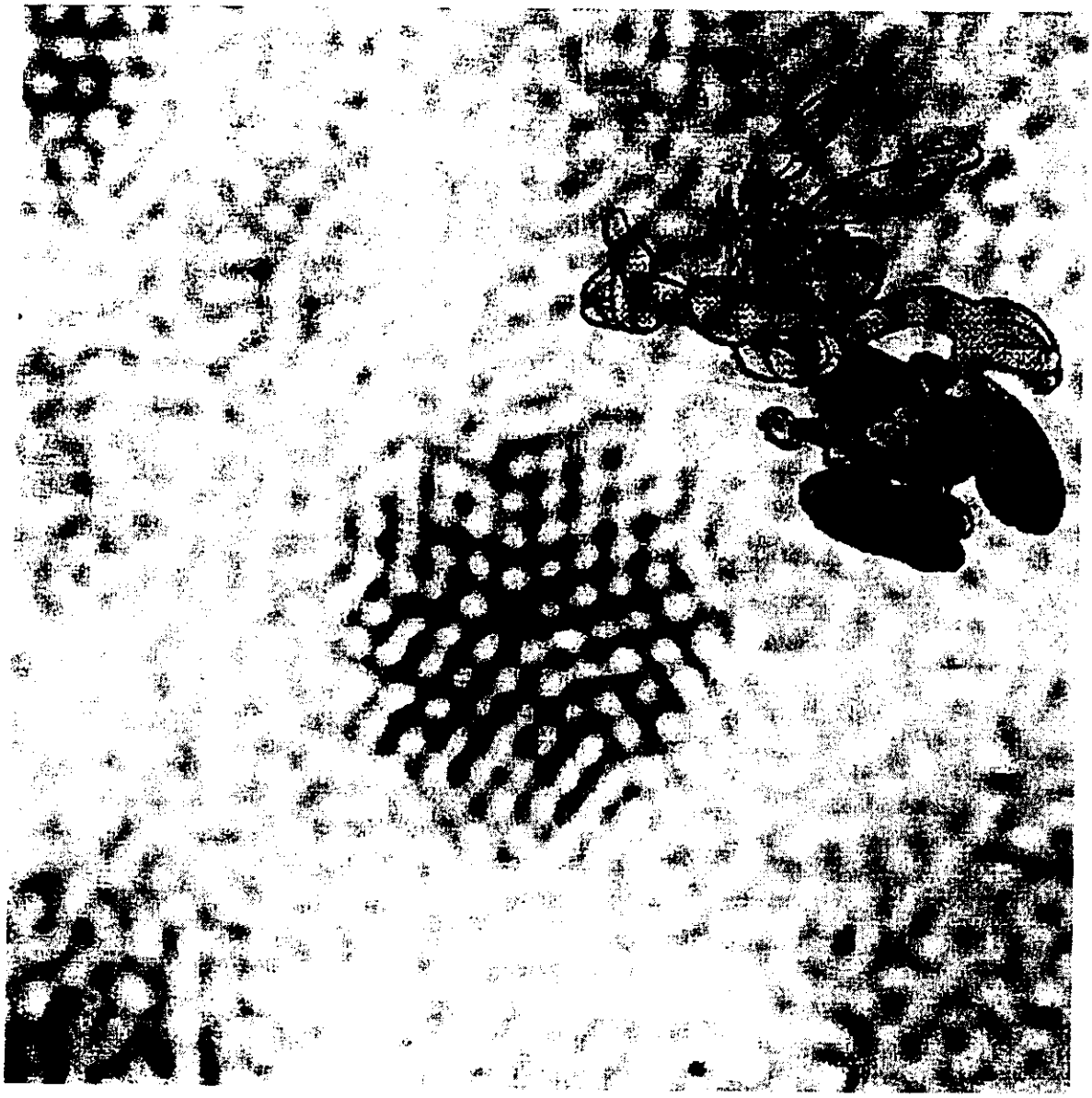

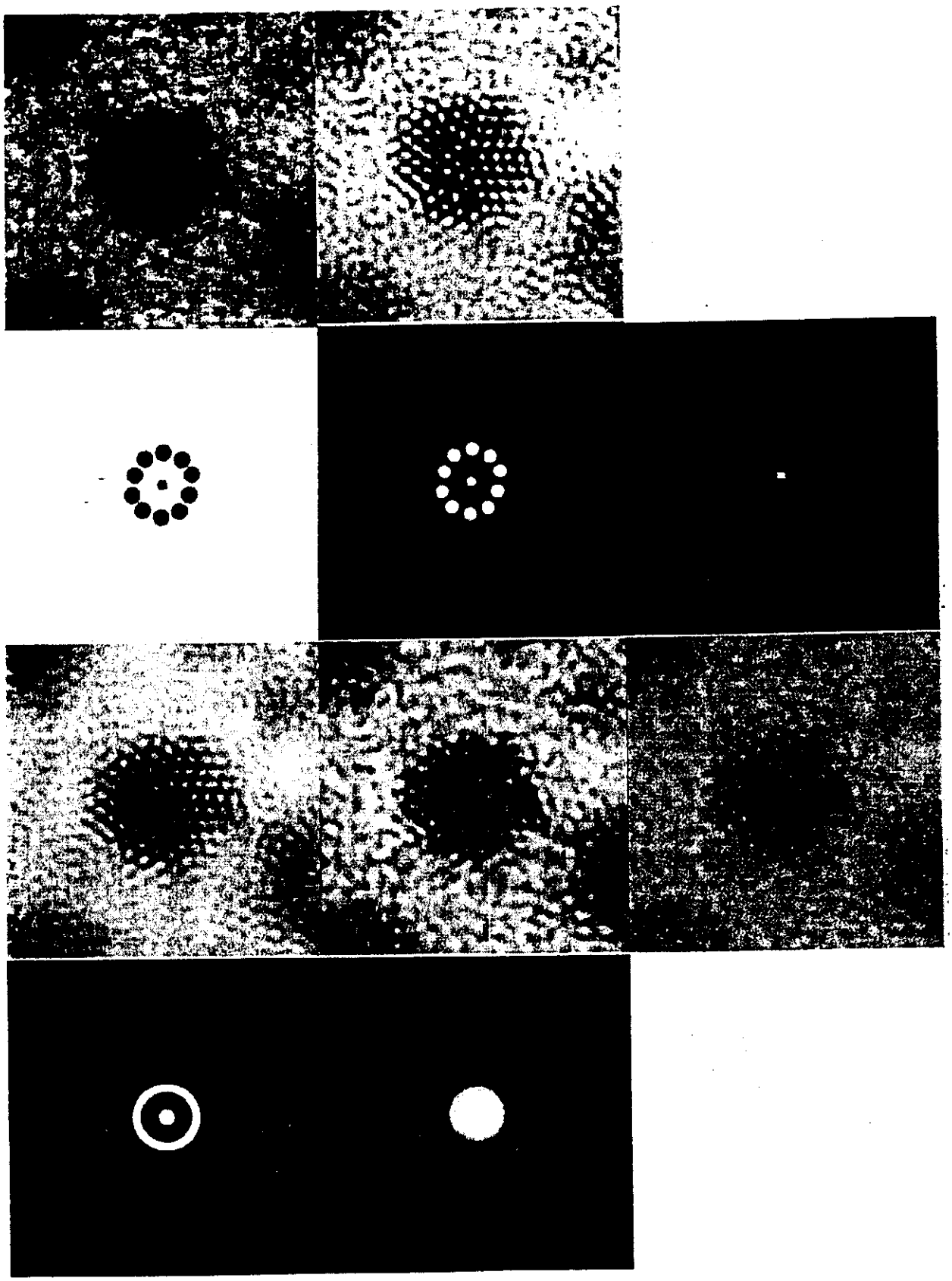

Electron Sample Interaction

Elastic

Inelastic

- X-Ray emission
- Slow secondary electrons
- Fast secondary electrons
- Auger electrons
- Electron-hole pairs
- Plasmons and phonons
- Radiolysis

Measured probe diameter and lattice image of carbon graphite

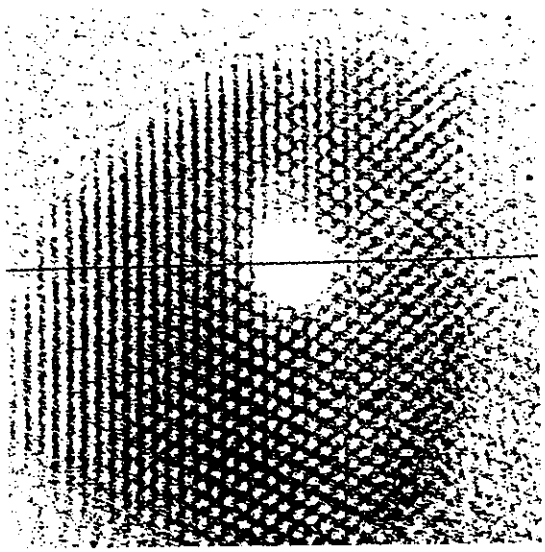

An electron probe focused on a specimen and an Au particle, which were photographed on the Imaging Plate (IP).

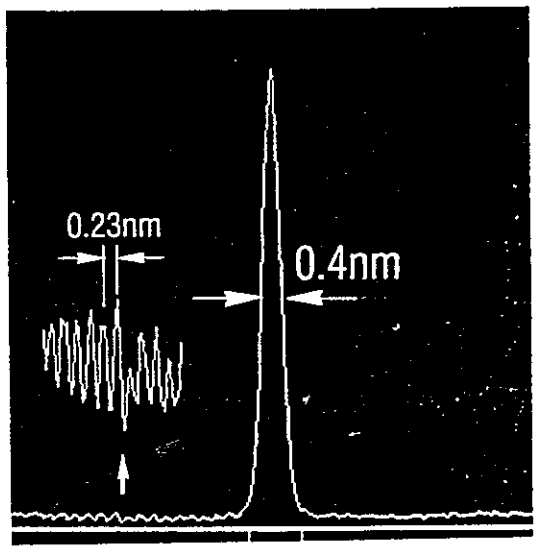

Profile on the line in the image at left

Probe diameter and specimen illumination current

Shown above is a micrograph showing a measured minimum probe diameter of 0.4 nm using an imaging plate with excellent linearity of electron sensitivity over a very wide range, to record the probe image. The probe size is in good agreement with the calculated value. There is sufficient probe current in this probe to provide effective analytical results with the highest possible spatial resolutioin.

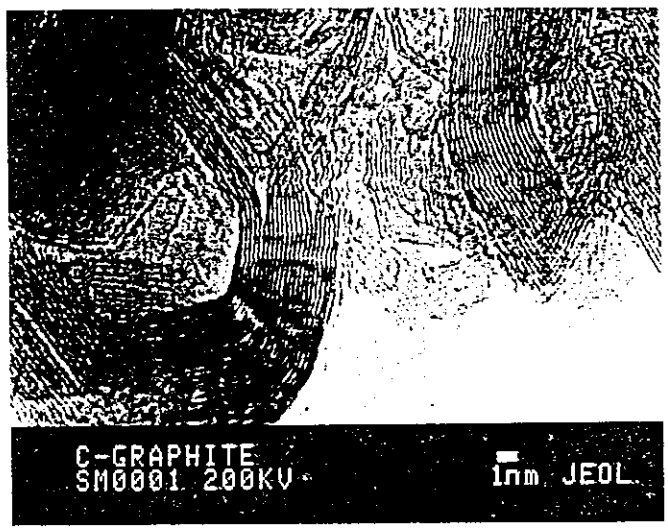

Shown above is an STEM image of carbon graphite, observed with the Scanning Image Observation Device. A lattice image of 0.34 nm is clearly observed, proving that the probe was this order of diameter.

Dr. M.J. Yacaman
U.N.A.M., Mexico

T95057
August 1995

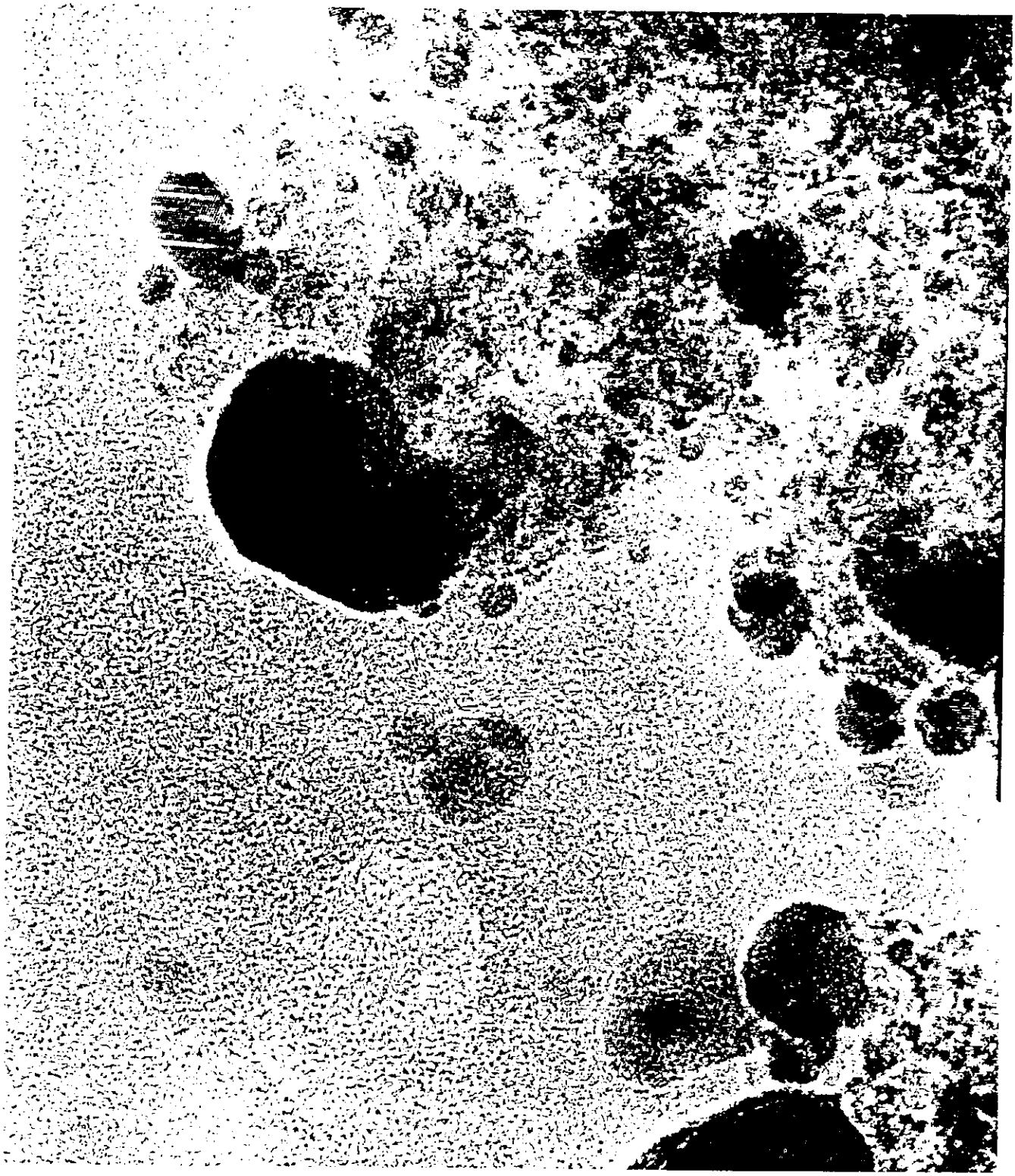

Magnification	:	2 030 000x	File code	:	W1117
El.Opt. Magn.	:	580 000x	High tension	:	200 kV
Microscope	:	CM200 FEG-SuperTWIN-α	Specimen	:	Pt-Ru on Al_2O_3

High-resolution image of Pt-Ru particles and substrate.

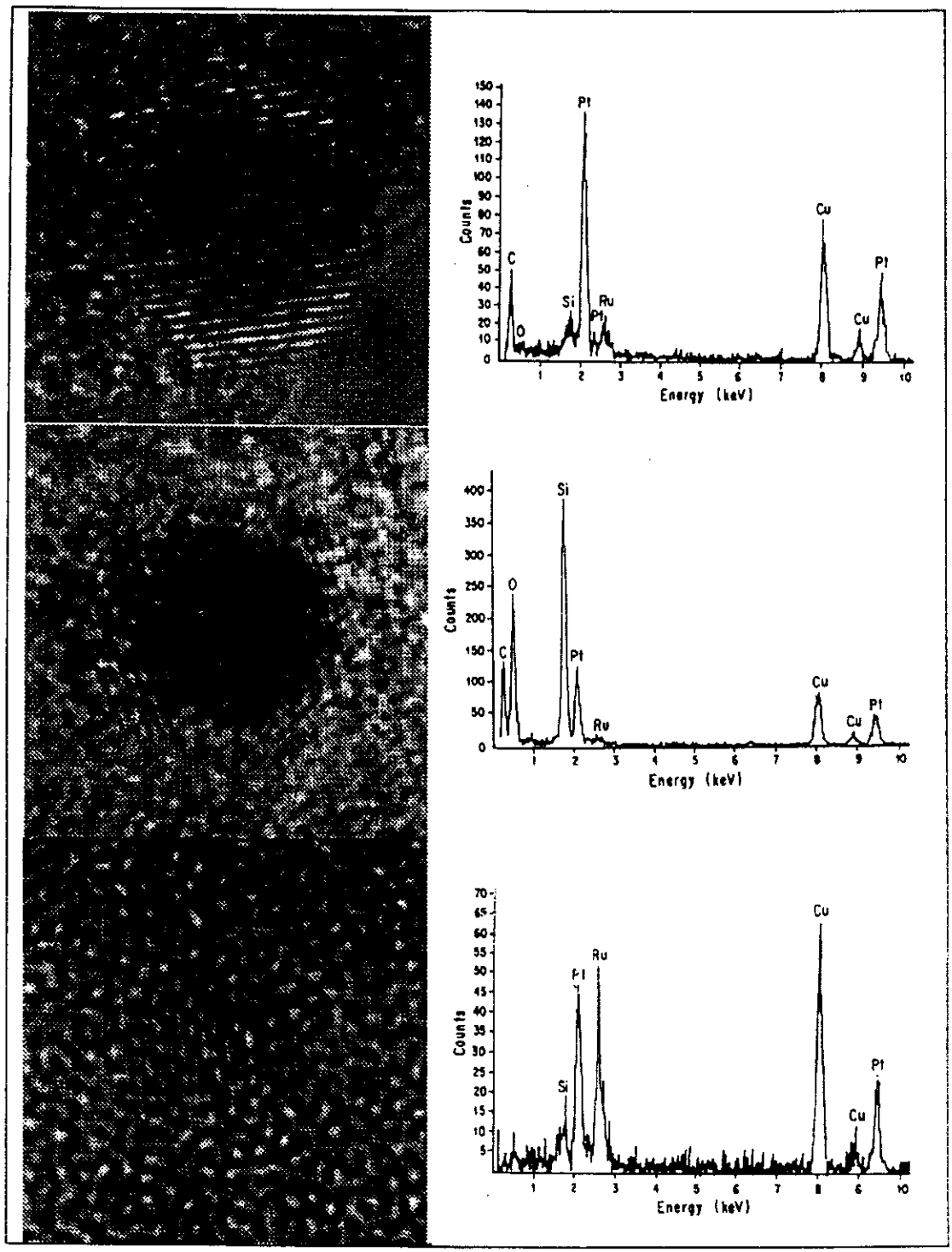

Figure 1) High resolution images of particles with its corresponding spectrum. Particle 1 and 2 correspond to Pt Rich and 3 to Ru Rich particles.

1 S. Alerasool and R. Gonzalez. J. of Catal. 124 (1990)204

2 R.E. Lakis et. al proc. of the 13th int. congress of Electron Microscopy, Paris (1994) 10750

3 M. José-Yacamán and M. Avalos. Catal. Rev. Scie and Eng. 34, 55-127(1992)

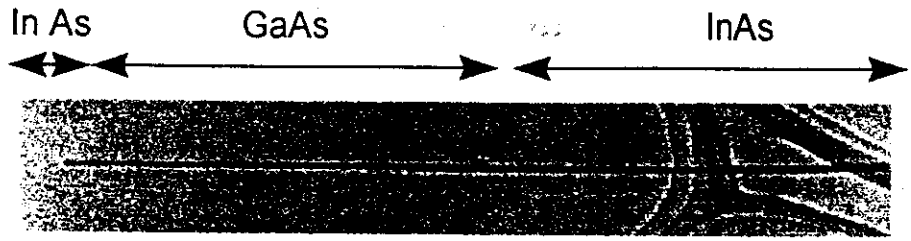

(a) TEM micrograph of a GaAs/InAs whisker

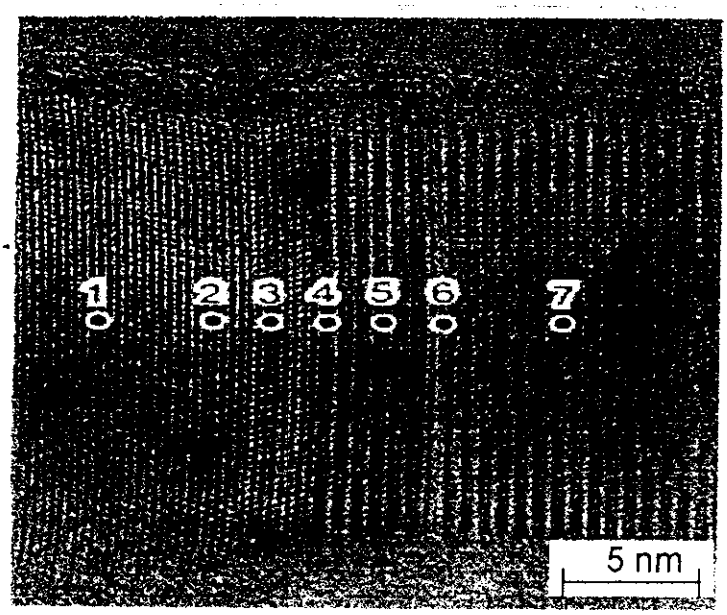

(b) HRTEM micrograph of a whisker around the GaAs/InAs hetero-interface

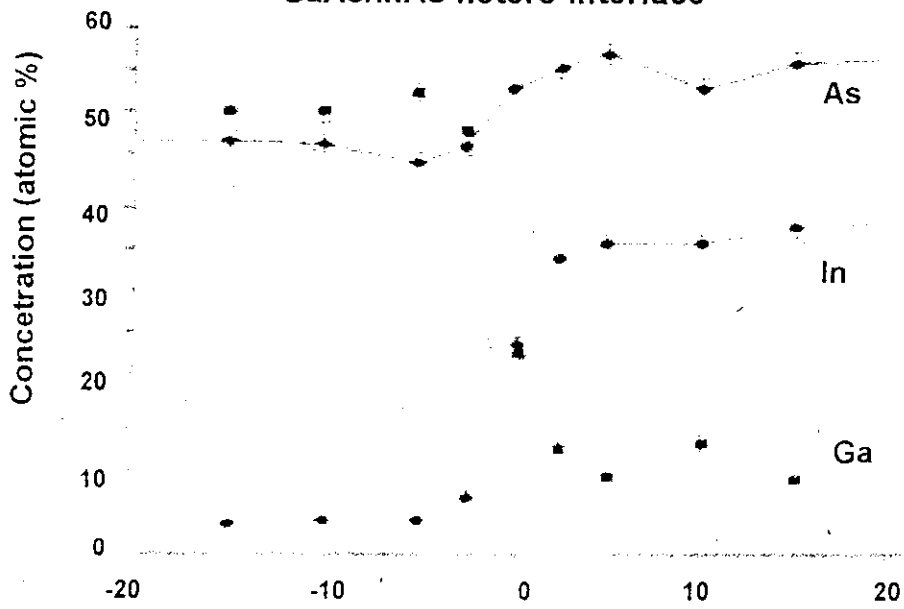

(c) Composition profiles around the GaAs/InAs hetero-interface

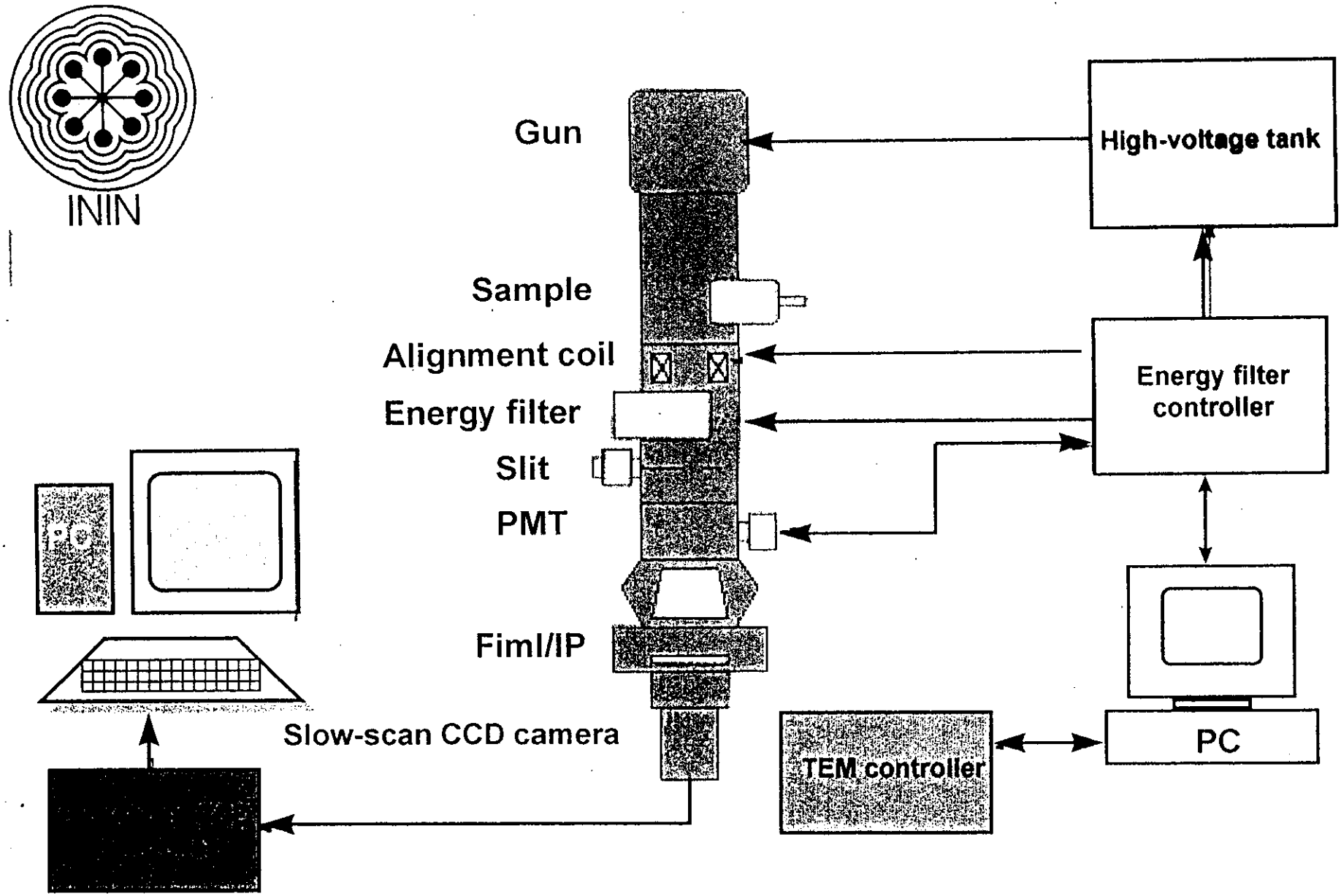
ININ
Gun
Sample
Alignment coil
Energy filter
Slit
PMT
Fiml/IP
Slow-scan CCD camera
High-voltage tank
Energy filter controller
TEM controller
PC

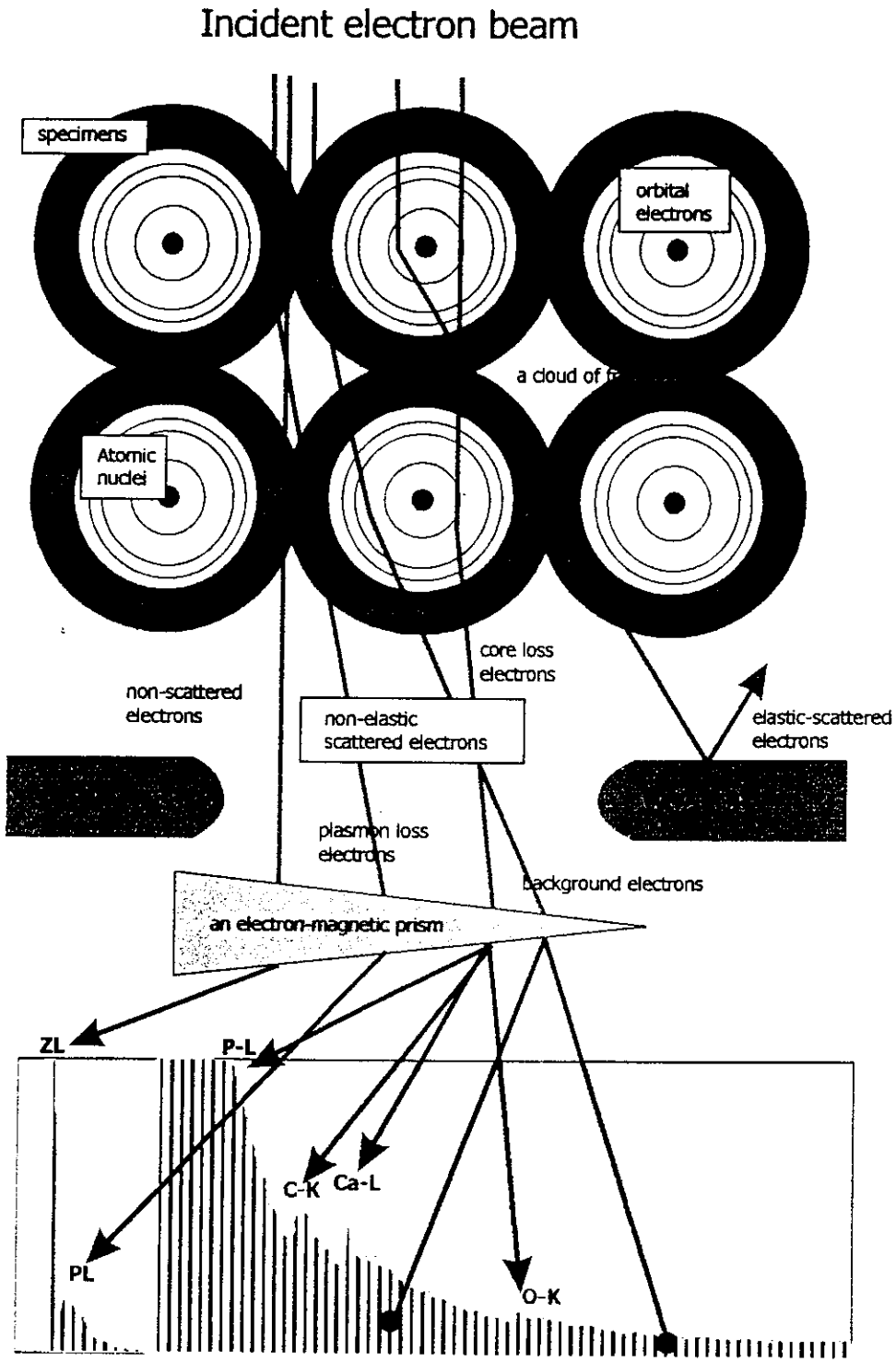

The principle of ESI

Type of Interaction	Energy Loss (eV)	Angle θ_E (mrads)
Electron - Phonon	- 0.02	5 - 15
Electron inter or intra band transitions	5 - 25	5 - 10
Electron - Plasmon	3 - 25	Less than 0.1
Inner shell ionization	10 - 1000	1 - 5

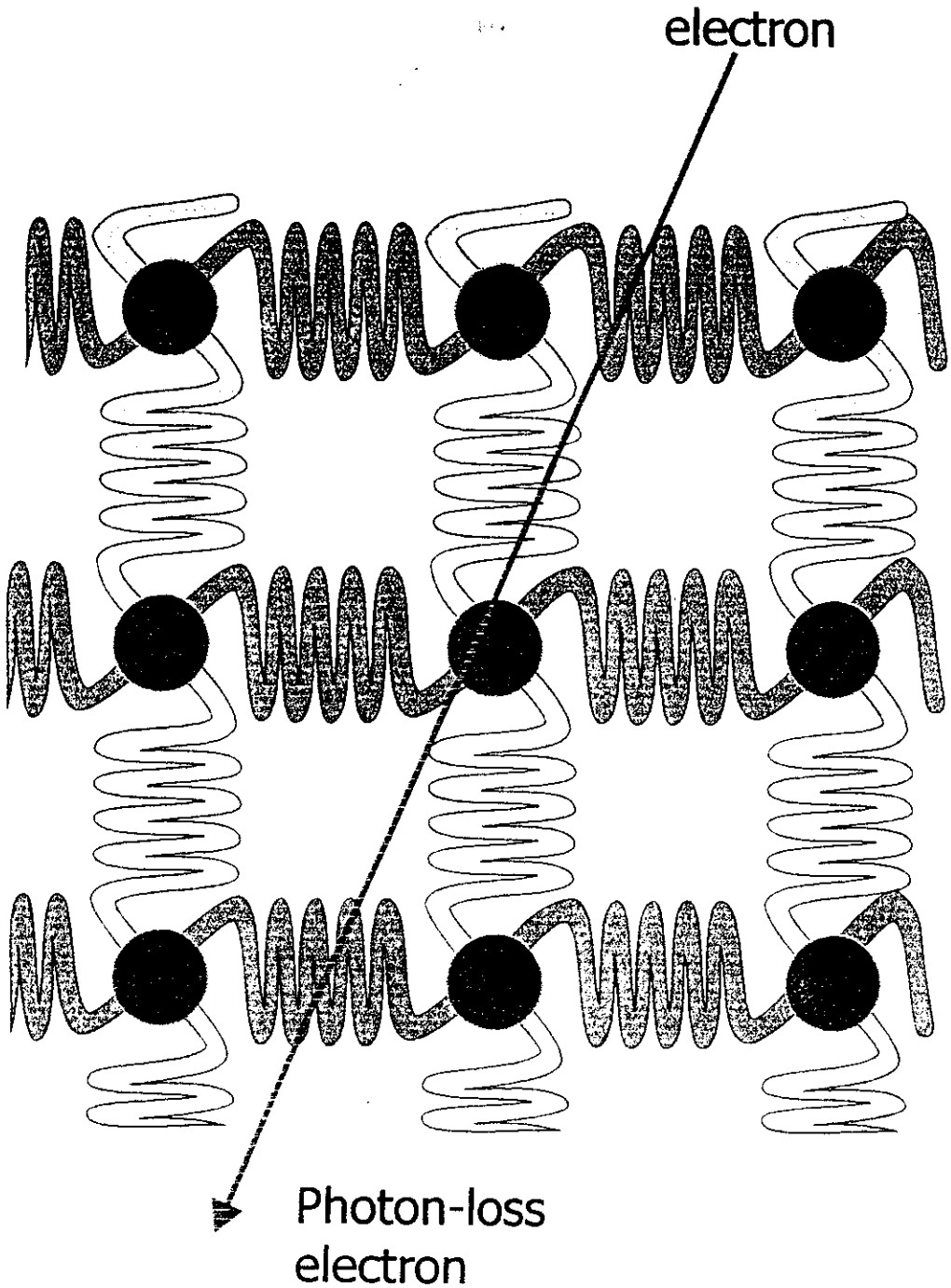

An illustration of the crystal lattice as a group of atoms linked elastically by springs. The bonds vibrate when struck by a high-energy electron creating lattice oscillations or phonons. The lattice absorbs heat by creating, so phonon excitation is equivalent to heating the specimen.

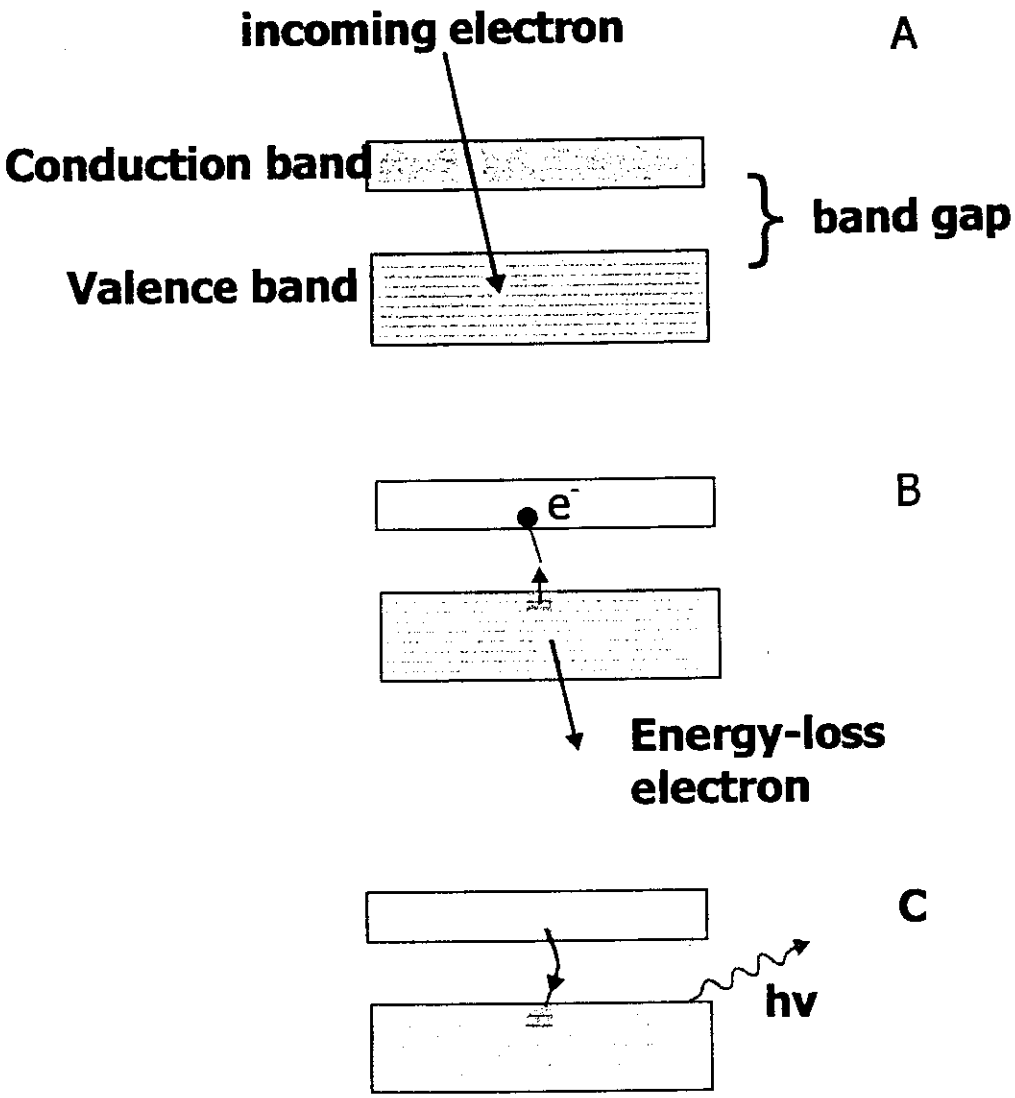

Schematic illustration of CL: (A) Initial state before a beam electron interacts with valence-band electrons. (B) A valence-band electron is excited across the gap into the conduction band, leaving a hole in the valence band. (C) The hole is filled by a conduction-band electron falling back into the valence-band hole. Upon recombination a photon of light is emitted, with a frequency determined by the band gap.

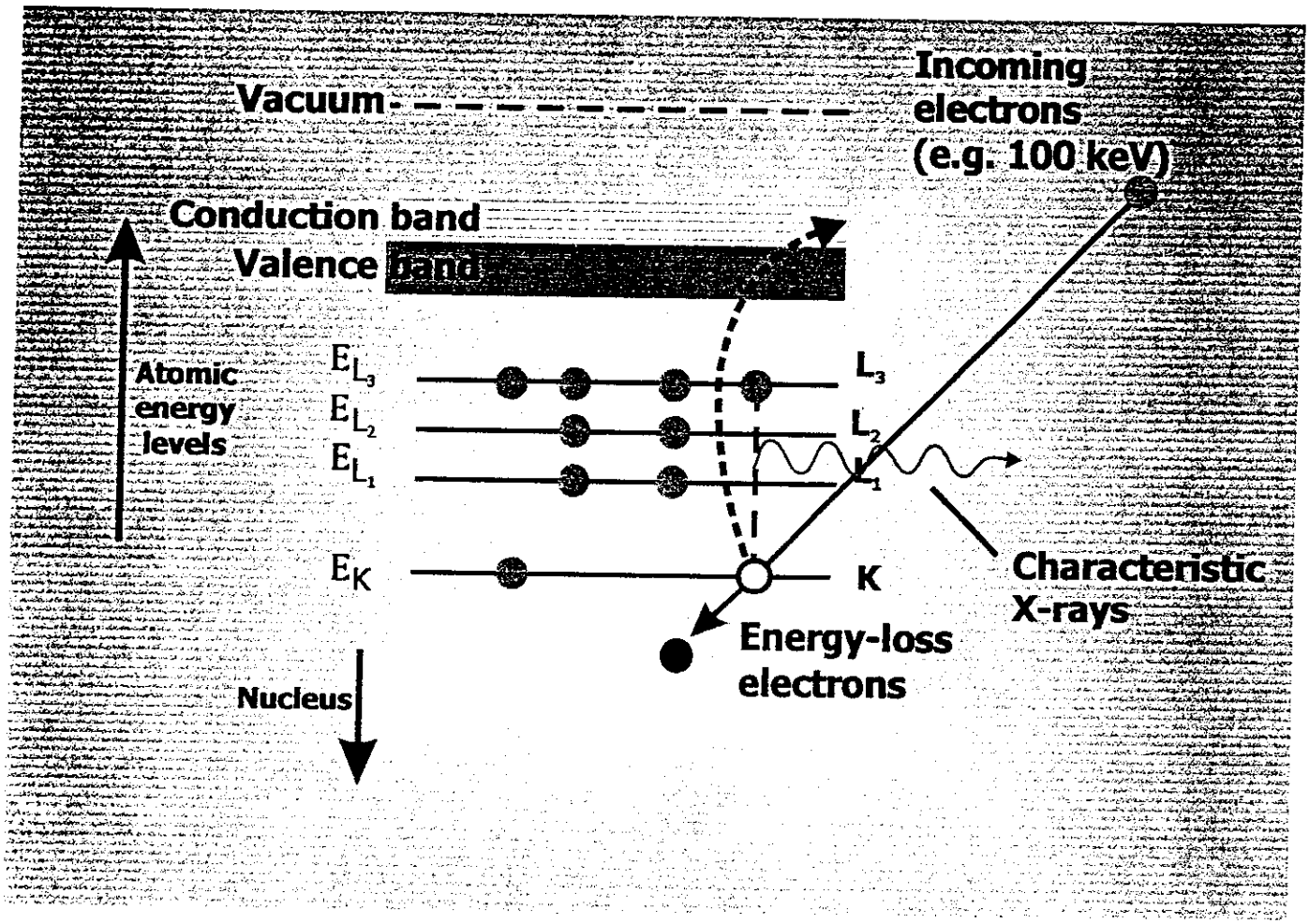

The ionization process. An inner (K) shell electron is ejected from the atom by a high-energy electron. When the hole in the K shell is filled by an electron from the L shell, characteristic K_α X-ray emission occurs. The beam electron loses energy but continues ion through the specimen.

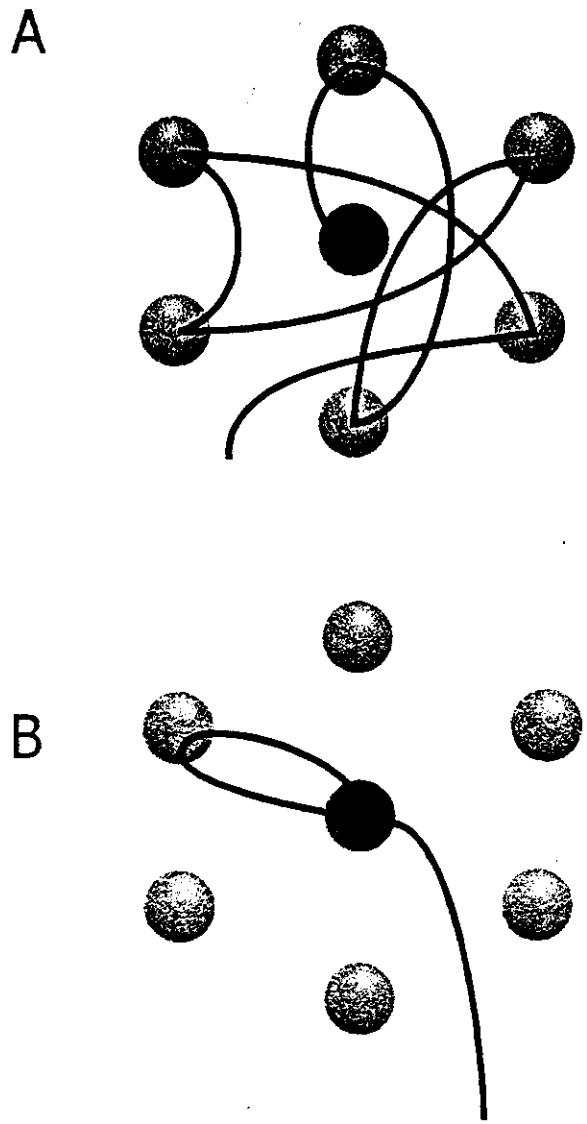

Schematic diagram of the source of (A) ELNES and (B) EXELFS. Excess energy above E_c creates a wave that is scattered by the sorrounding atoms. The low-energy ELNES arises from plural scatter and the higher energy EXELFS from single scatter.

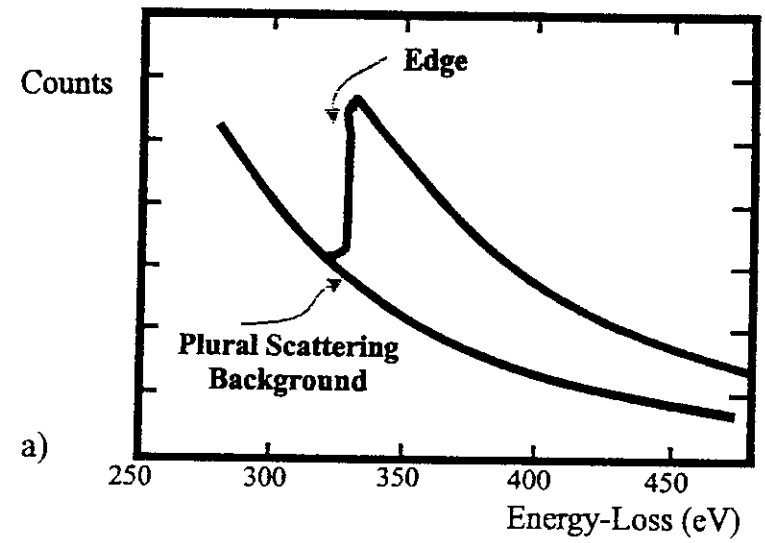
Counts
Edge
Plural Scattering
Background
a)
250
300
350
400
450
Energy-Loss (eV)

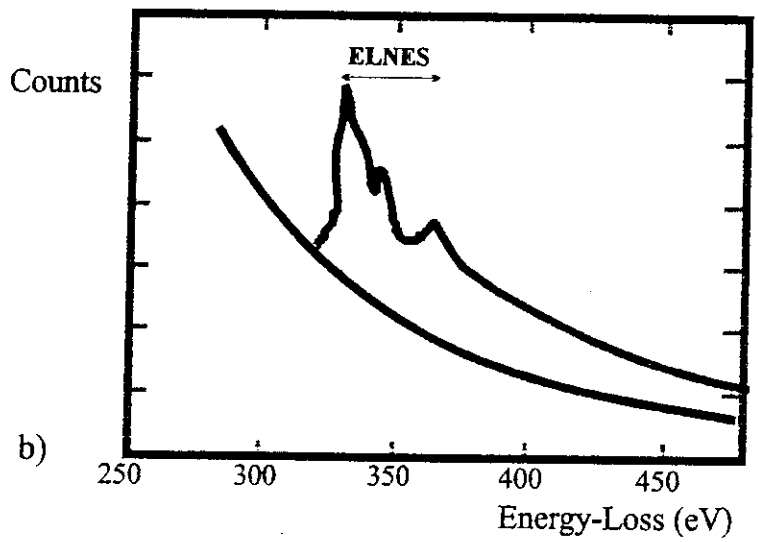
Counts
ELNES
b)
250
300
350
400
450
Energy-Loss (eV)

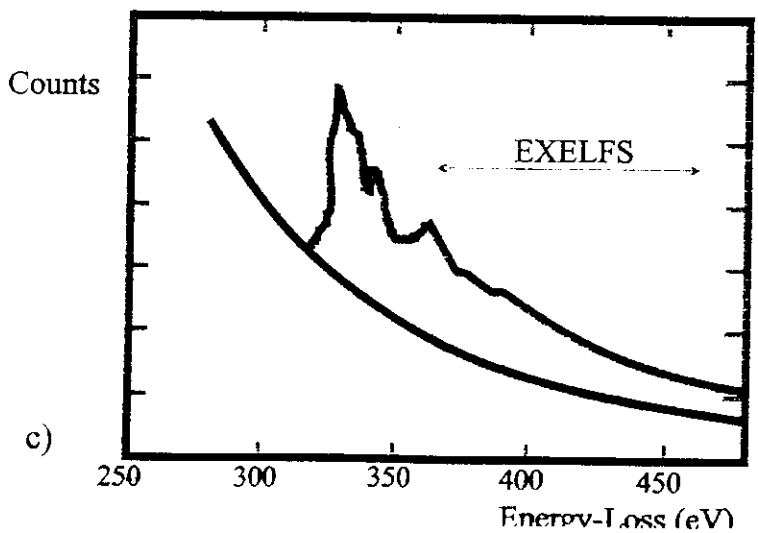
Counts
EXELFS
c)
250
300
350
400
450
Energy-Loss (eV)

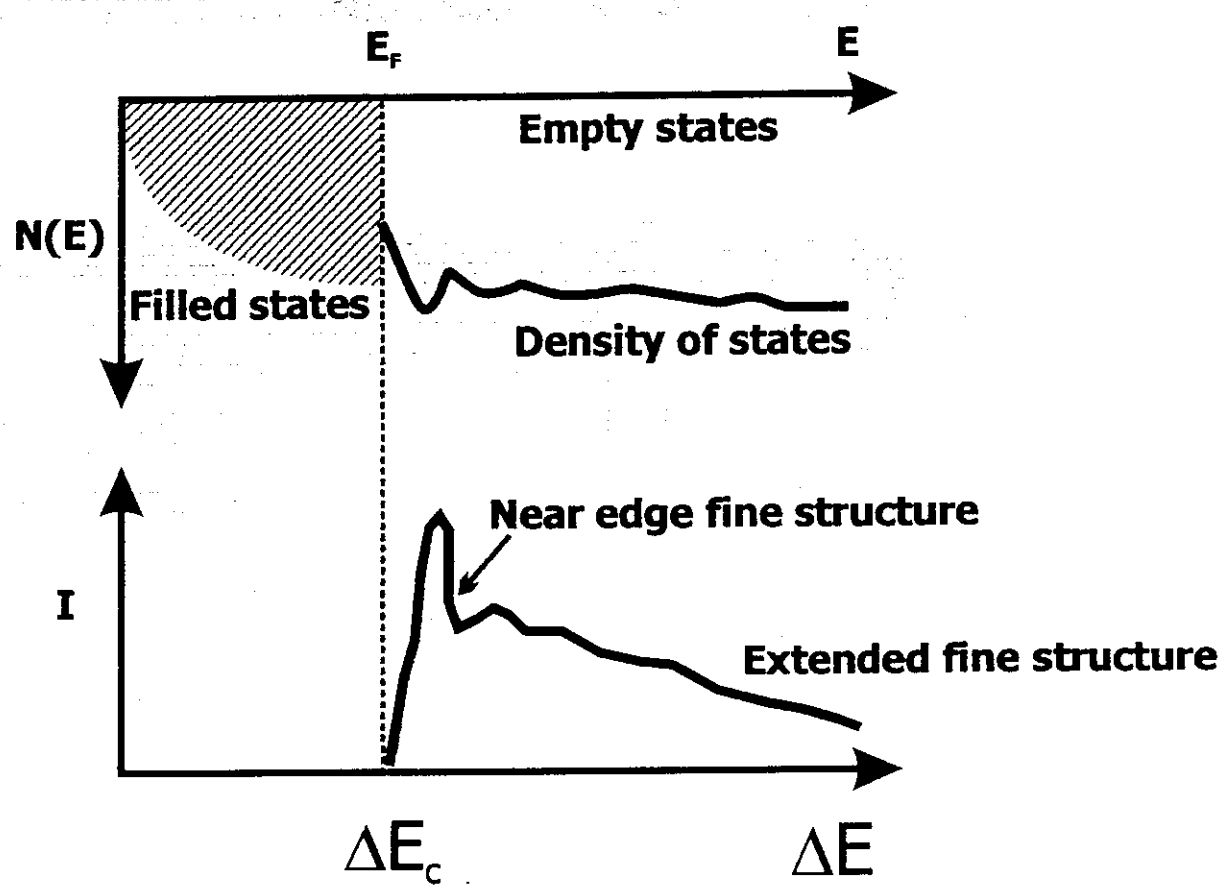

The relationship between the ELNES and the unfilled density of states

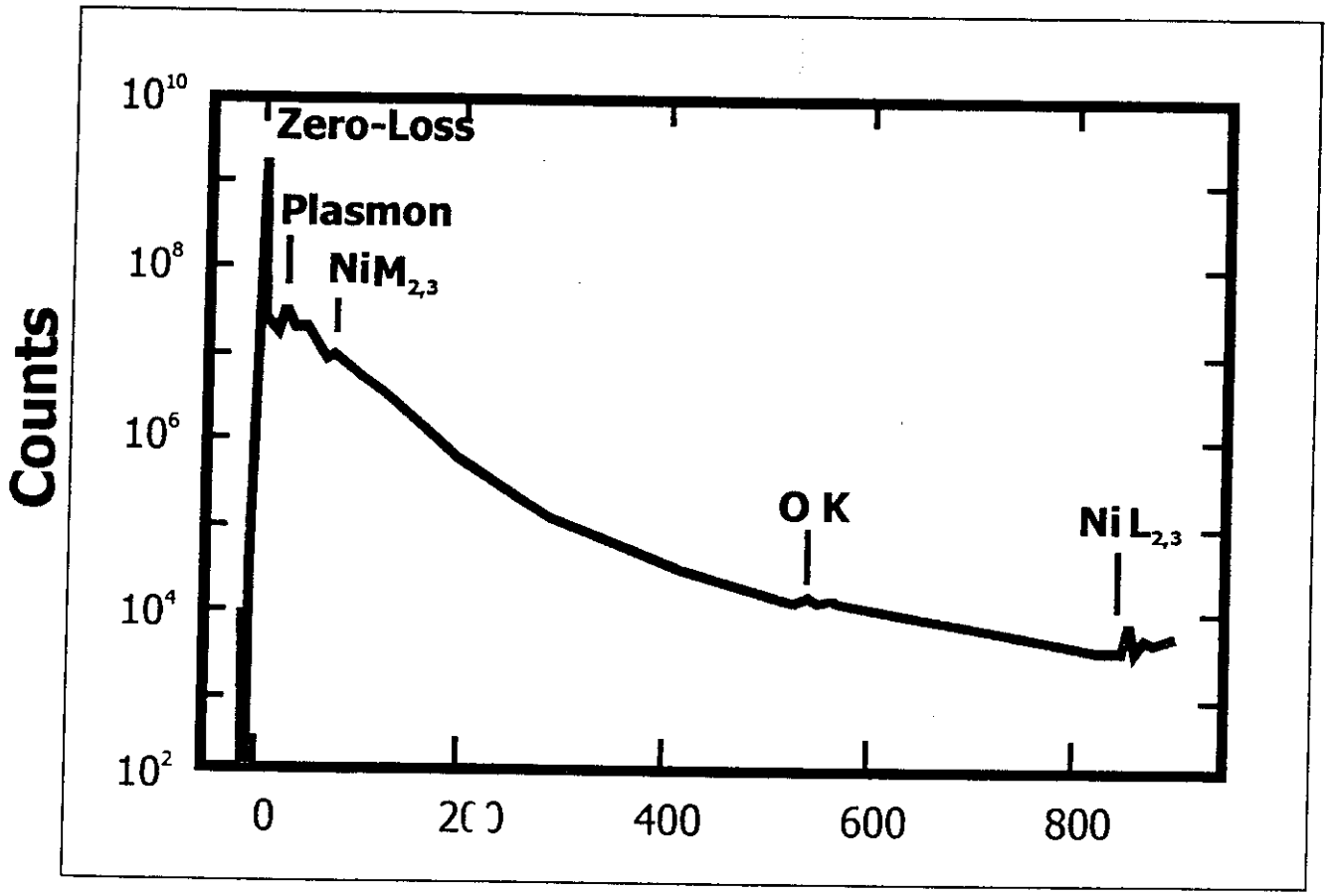

EELS spectrum from NiO showing the many orders of magnitude difference in intensity from the zero-loss peak to the fine structure.

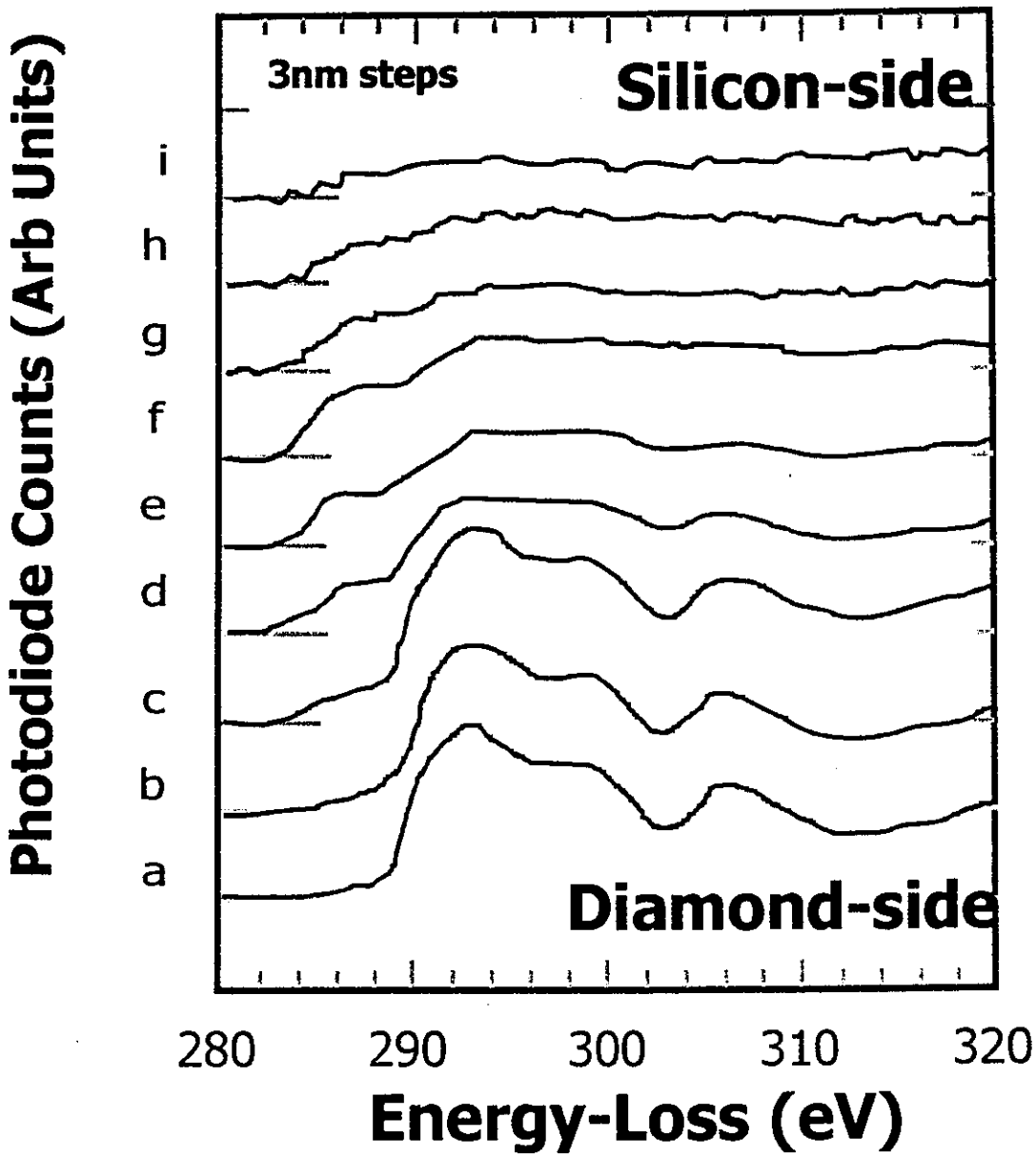

Spectrum-line profile across the interfaces between a diamond-like carbon film, an amorphous carbon interlayer and a Si substrate.

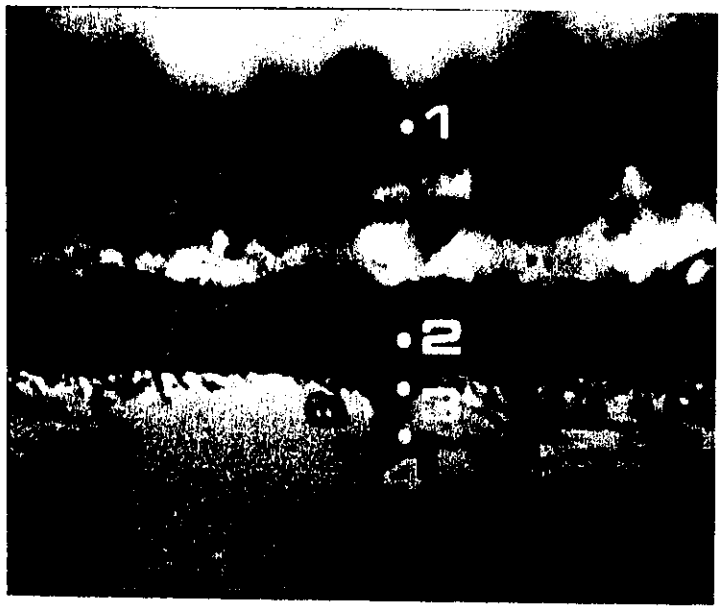

Table 1: Atomic concentrations of Al, Si and Ti in the Al/TiN/Si layer of Ti60 specimens after the heating test. The identification numbers of the analyzed regions are indicated in figure.

ANALYZED REGION	Al	Si	Ti	Position
1	97	3	<1	Top Al Layer
2	17	60	23	TiN film
3	4	94	2	Defective layer on the upper part of p-type Si substrate
4	2	98	<1	Dislocation band in Si p-region

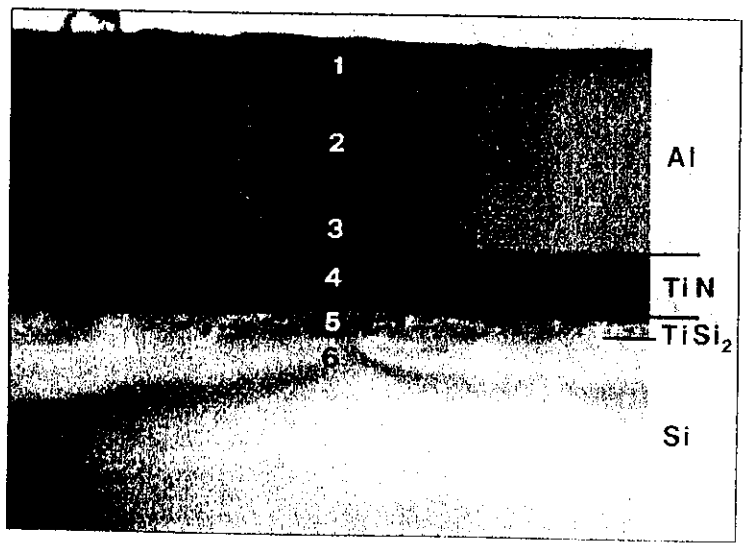

Table2: Atomic concentrations of Al, Si and Ti in the Al/TiN/$TiSi_2$/Si layer of Ti100 specimens after the heating test. The identification numbers of the analyzed regions are indicated in figure.

ANALYZED REGION	Al	Si	Ti	Position
1	99	1	<1	Top Al layer
2	99	1	<1	Center of Al layer
3	98	2	<1	Bottom of Al layer
4	9	24	67	TiN film
5	2	74	24	$TiSi_2$ film
6	2	98	<1	Si p-region

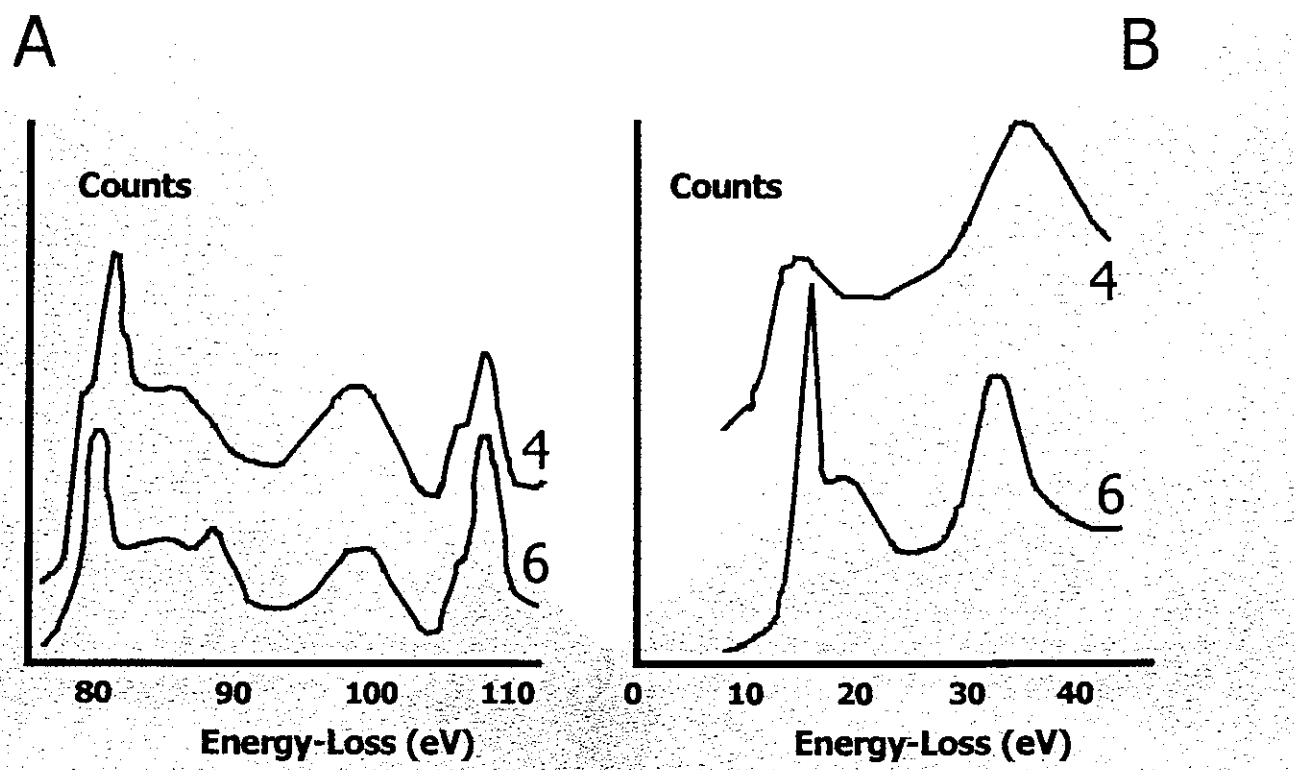

Comparison of (A) experimental and (B) calculated ELNES for Al in minerals with coordination numbers of 4 and 6 respectively.

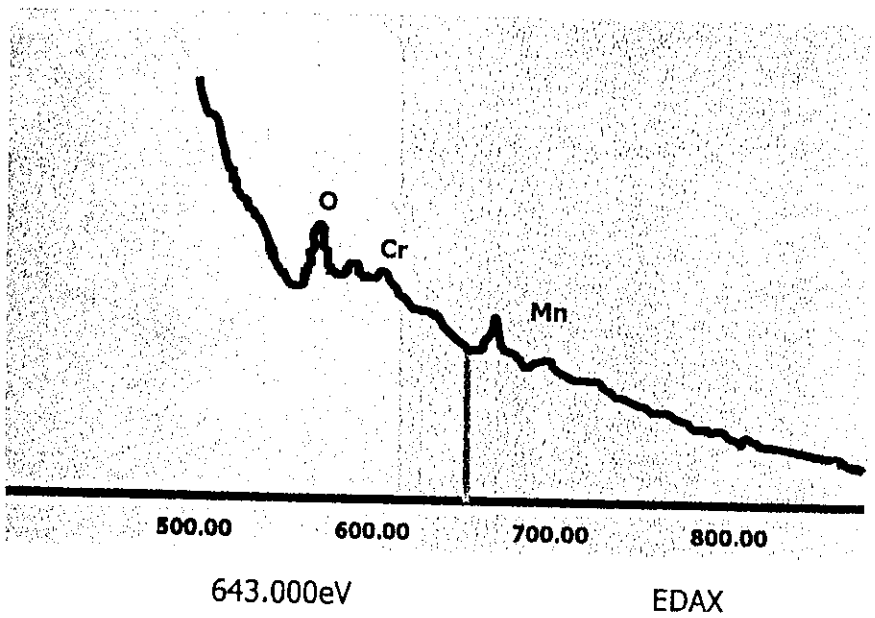

EELS spectrum from the small oxide inclusion A in the Cr_2N particle shown in image.

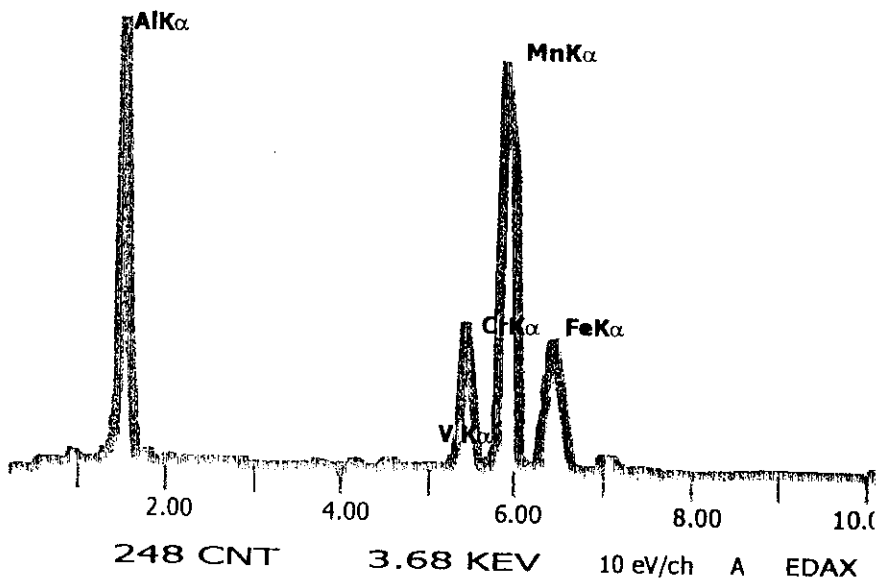

EDS spectrum form the small oxide inclusion A in the Cr_2N particle shown in image.